

Copyright  
by  
Watsamon Sahasakkul  
2014

The Thesis Committee for Watsamon Sahasakkul  
Certifies that this is the approved version of the following thesis:

**Development of a Model for  
an Offshore Wind Turbine Supported by  
a Moored Semi-Submersible Platform**

**APPROVED BY  
SUPERVISING COMMITTEE:**

---

Lance Manuel, Supervisor

---

Loukas F. Kallivokas

**Development of a Model for  
an Offshore Wind Turbine Supported by  
a Moored Semi-Submersible Platform**

**by**

**Watsamon Sahasakkul, B.E.**

**THESIS**

Presented to the Faculty of the Graduate School of  
The University of Texas at Austin  
in Partial Fulfillment  
of the Requirements  
for the Degree of

**Master of Science in Engineering**

THE UNIVERSITY OF TEXAS AT AUSTIN

August 2014

Dedicated to my parents, my sister and brother.

## Acknowledgments

First of all, I wish to express my appreciation to my advisor, Dr. Lance Manuel, for his encouragement, guidance, and patience. His help and contribution of time is appreciated. He provided many helpful suggestions and comments for improving the work. I thank member of my thesis committee, Dr. Loukas F. Kallivokas for serving on my committee.

I would also like to thank Mr. Mohit Soni for being a great colleague to get started and solve many problems on this research. I also thank Mr. Eungsoo Kim for helpful comments on getting started with simulation. In addition, I would like to thank Dr. Jason Jonkman and others from the National Renewable Energy Laboratory the simulation tools, FAST and TurbSim, that were used in this study. I also thank Dr. Todd (Daniel) Griffith, Dr. Matthew Barone and Ms. Kelly Ruehl from Sandia National Laboratories for providing us with the wind turbine model used in this study and for assistance in modeling the offshore platform.

The financial support from Sandia National Laboratories by way of Contract No. 1307455 is acknowledged.

Last but not least, I would like to share this success and thank my parents, brother, and sister for their unconditional love and support. Without them, I would never finish this work.

## **Abstract**

### **Development of a Model for an Offshore Wind Turbine Supported by a Moored Semi-Submersible Platform**

Watsamon Sahasakkul, M.S.E.

The University of Texas at Austin, 2014

Supervisor: Lance Manuel

Wind energy is one of the fastest growing sources of renewable energy in the world. There has been a lot of research, development, and investment in wind energy in recent years. Offshore sites offer stronger winds and low turbulence, along with fewer noise and visual impacts. Establishing large turbines at deepwater sites offers promising opportunities for generating high power output while utilizing the favorable environmental conditions. Researchers at Sandia National Laboratories (SNL) have developed a very large wind turbine model with a 13.2 MW rating that has 100-meter long blades; this turbine is designated as the SNL100 13.2 MW wind turbine. With a hub height of 146 meters and a rotor diameter of 205 meters, such a

large turbine is best suited for offshore sites. Developing a wind turbine model for an offshore site requires that a platform model be developed first. Of the various kinds of floating platforms, a moored semi-submersible platform supporting the wind turbine, which offers stability by virtue of the intercepted water-plane area, is an appropriate choice. The goal of this study is to develop a semi-submersible platform model to support the 13.2 MW wind turbine, while keeping loads and deflections within safe limits.

The platform is developed based on work completed as part of the Offshore Code Comparison Collaboration Continuation (OC4) Phase II project, which involved a 5 MW wind turbine supported by a semi-submersible platform. The present study focuses on three important topics: (i) development of the combined offshore wind turbine system model with the 13.2 MW wind turbine, a floating semi-submersible platform, and a mooring system; (ii) the entire procedure involved in modeling and analyzing first-order hydrodynamics using two codes, MultiSurf and WAMIT; and (iii) assembling of the integrated aero-hydro-servo-elastic model considering hydrodynamics in order to verify the steady-state and stochastic response of the integrated wind turbine system.

# Table of Contents

<b>Acknowledgments</b>	<b>v</b>
<b>Abstract</b>	<b>vi</b>
<b>List of Tables</b>	<b>xi</b>
<b>List of Figures</b>	<b>xii</b>
<b>Chapter 1. Introduction</b>	<b>1</b>
1.1 Background . . . . .	1
1.2 Research Objectives and Methodology . . . . .	2
1.2.1 Model Development for the Floating Offshore Wind Turbine	3
1.2.2 Semi-submersible Platform Hydrodynamics . . . . .	3
1.2.3 Steady-state and Stochastic Responses of the Integrated Turbine-Platform-Mooring System . . . . .	4
1.3 Limitations . . . . .	4
1.4 Organization of Thesis . . . . .	5
<b>Chapter 2. Model Development for a                 Floating Offshore Wind Turbine</b>	<b>7</b>
2.1 Floating Wind Turbine Concepts . . . . .	8
2.2 Simulation Tools for Model Development . . . . .	11
2.2.1 FAST . . . . .	12
2.2.2 TurbSIM . . . . .	14
2.2.3 WAMIT . . . . .	14
2.2.4 MultiSurf . . . . .	15
2.3 SNL 13.2 MW Wind Turbine Model . . . . .	15
2.3.1 Blade Structural Properties . . . . .	17
2.3.2 Tower Structural Properties . . . . .	20



2.3.3	Steady-State Response to Uniform Non-Turbulent Wind	22
2.3.4	Control System for the 13.2 MW Offshore Wind Turbine	26
2.4	Semisubmersible Platform . . . . .	27
2.4.1	Platform Coordinate System . . . . .	30
2.5	Catenary Mooring System . . . . .	31
<b>Chapter 3.</b>	<b>Semi-submersible Platform Model Hydrodynamics</b>	<b>35</b>
3.1	Hydrodynamic Loading on the Floating Platform . . . . .	38
3.2	Analysis using WAMIT . . . . .	41
3.3	Use of WAMIT . . . . .	43
3.3.1	Model.gdf . . . . .	44
3.3.2	Model.pot . . . . .	44
3.3.3	Model.frc . . . . .	46
3.3.4	config.wam and Model.cfg . . . . .	46
3.3.5	fnames.wam . . . . .	46
3.4	Use of MultiSurf . . . . .	47
3.5	Linear Hydrodynamic Analysis Results from WAMIT . . . . .	50
3.5.1	Added Mass . . . . .	51
3.5.2	Radiation Damping . . . . .	53
3.5.3	Hydrodynamic wave excitation forces . . . . .	56
3.6	WAMIT and MultiSurf Files . . . . .	56
<b>Chapter 4.</b>	<b>Response Analyses for the OC4 5 MW and the 13.2 MW Wind Turbines</b>	<b>58</b>
4.1	Important Modeling Considerations . . . . .	59
4.1.1	Linear hydrodynamics with potential flow . . . . .	59
4.1.2	Nonlinear Hydrodynamics . . . . .	60
4.2	Steady-State Response of the Semi-Submersible Platform under Regular Waves . . . . .	61
4.2.1	Steady-State Platform Motion Time Series . . . . .	62
4.2.2	RAOs for Motions of the OC4 5 MW Turbine and the 13.2 MW Turbine Semi-Submersible Platforms . . . . .	66
4.3	Response of 13.2 MW Turbine to Irregular Waves and Turbulent Wind Fields . . . . .	69

4.4	TurbSim and FAST Files . . . . .	74
4.5	Summary . . . . .	74
<b>Chapter 5.</b>	<b>Conclusions</b>	<b>75</b>
5.1	Overview of the Research Study . . . . .	75
5.2	Conclusions . . . . .	76
5.3	Suggestions for Future Research . . . . .	78
<b>Appendix</b>		<b>80</b>
<b>Appendix A.</b>	<b>Model Files</b>	<b>81</b>
A.1	MultiSurf Output Files for WAMIT . . . . .	81
A.2	Additional WAMIT Input Files . . . . .	82
A.3	Sample of WAMIT Output Files for HydroDyn Inputs . . . . .	82
A.4	TurbSim Input File . . . . .	85
A.5	FAST Input Files . . . . .	86
A.5.1	FAST . . . . .	86
A.5.2	AeroDyn . . . . .	87
A.5.3	ServoDyn . . . . .	88
A.5.4	ElastoDyn . . . . .	89
A.5.5	Blade File for ElastoDyn . . . . .	92
A.5.6	Tower File for ElastoDyn . . . . .	93
A.5.7	HydroDyn . . . . .	94
A.5.8	MAP . . . . .	98
<b>Bibliography</b>		<b>99</b>
<b>Vita</b>		<b>105</b>

## List of Tables

2.1	Properties of the 13.2 MW baseline turbine model. . . . .	16
2.2	Properties of the three 100-meter blade models. . . . .	17
2.3	Blade pitch controller parameters employed in the OC4 project [1].	26
2.4	Variable speed controller parameters. . . . .	27
2.5	Scaling relationships for development of the platform model [2].	29
2.6	Properties and dimensions of the semi-submersible platform. .	30
2.7	Mooring system properties. . . . .	34
3.1	Number of panels for the symmetric half model of the platform.	50
4.1	Surge and pitch natural frequencies for the semi-submersible platform models. . . . .	69

## List of Figures

2.1	Floating offshore wind turbine concepts classified based upon how they provide stability [3]. . . . .	10
2.2	Simulation tools and modules for the integrated turbine, platform, and mooring system. . . . .	12
2.3	Currently used and proposed blade lengths [4]. . . . .	16
2.4	Three views of the blade surface geometry: flapwise, edgewise, and isometric [5]. . . . .	18
2.5	Variation in mass density, flapwise stiffness, and edgewise stiffness along the length for the three 100-meter blades. . . .	19
2.6	Flapwise and edgewise mode shapes for the three 100-meter blades. . . . .	20
2.7	Variation of mass density and stiffnesses along the height of the tower. . . . .	21
2.8	Fore-aft and side-to-side tower mode shapes. . . . .	22
2.9	Steady-state response of the 13.2 MW wind turbine as a function of hub-height wind speed: tip-speed ratio, blade pitch angle, generator power, and rotor power. . . . .	24
2.10	Steady-state response of the 13.2 MW wind turbine as a function of hub-height wind speed: generator speed, rotor speed, generator torque, rotor torque, and rotor thrust. . . . .	25
2.11	The semi-submersible platform model showing structural components [1]. . . . .	29
2.12	Reference coordinate system for the floating platform (illustrated for a barge platform) [6]. . . . .	31
2.13	The catenary mooring line system for the semi-submersible platform [7]. . . . .	33
3.1	Flow chart for obtaining desired hydrodynamic coefficients (FAST inputs for the HydroDyn module). . . . .	37
3.2	Linear hydrodynamic effects illustrated for a vertical cylinder [6].	38
3.3	Flow chart showing various files involved in a WAMIT analysis [8].	45

3.4	Different views of the MultiSurf model and mesh for the semi-submersible platform. . . . .	48
3.5	MultiSurf models with division and subdivision meshes for the semisubmersible platform. . . . .	49
3.6	Added mass coefficients for the six degrees of freedom of the semi-submersible platform. . . . .	52
3.7	Wave-radiation damping coefficients for the six degrees of freedom of the semi-submersible platform. . . . .	54
3.8	Hydrodynamic added mass and radiation damping coefficients for coupled modes of the semi-submersible platform. . . . .	55
3.9	Wave excitation forces for the six degrees of freedom of the semi-submersible platform. . . . .	57
4.1	Time series of the OC4 platform steady-state response for a unit-amplitude wave at the surge natural frequency. . . . .	63
4.2	Time series of the OC4 platform steady-state response for a unit-amplitude wave at the pitch natural frequency. . . . .	64
4.3	RAOs for surge and pitch motions for the OC4 semi-submersible platform. . . . .	67
4.4	RAOs for surge and pitch motions for the 13.2 MW turbine semi-submersible platform. . . . .	68
4.5	Time series highlighting 10-minute segments of the simulated response of the 13.2 MW wind turbine-platform-mooring system given $V_{hub} = 23$ m/s, $H_s = 5.5$ m, and $T_p = 11$ s. . . . .	72
4.6	One-hour time series of the simulated response of the 13.2 MW wind turbine-platform-mooring system given $V_{hub} = 23$ m/s, $H_s = 5.5$ m, and $T_p = 11$ s. . . . .	73

# Chapter 1

## Introduction

### 1.1 Background

Over the past few decades, wind energy has grown significantly as a source of renewable energy. Still, over 75 percent of energy produced in the United States is from non-renewable sources including natural gas, coal, and crude oil [9]. To meet future energy demands, wind power is expected to play a significant part. Offshore wind energy, specifically, still in an early stage of development, has the potential to become a major contributor of renewable energy. According to the European Wind Energy Association (EWEA), Europe has, to date, 224 offshore wind turbines in 16 commercial wind farms, with an additional 310 wind turbines awaiting installation in 2014 [10]. The total capacity from all the offshore wind farms under construction in Europe in 2014 is expected to be over 4,900 MW. Similarly, in the U.S., according to Department of Energy (DOE) projections, offshore wind turbines are expected to contribute about 54 GW of offshore wind power by 2030 [11].

Offshore sites offer several advantages over sites on land—stronger winds, less turbulence, and relatively fewer visual and noise impacts. There is particular interest in offshore wind energy from available deepwater sites

where floating platforms are needed to support wind turbines. There are several kinds of offshore platforms that are suitable for supporting wind turbines in deep water; these are distinguished by the manner in which they achieve stability. One design concept involves the use of a semi-submersible platform. Researchers at the National Renewable Energy Laboratory (NREL) have developed a 5 MW baseline offshore wind turbine supported on a semi-submersible platform as part of the OC4 Phase II DeepCwind project [1]. That model has been developed using aero-hydro-servo-elastic codes that incorporate several features not considered in bottom-supported offshore wind turbines.

Researchers at Sandia National Laboratories have developed a 13.2 MW wind turbine with 100-meter blades; this turbine model is part of ongoing research studies [12]. In the present study, a preliminary model of a semi-submersible platform is developed for the 13.2 MW turbine for use at an offshore site; the platform model is based upon the OC4 platform. The behavior of this turbine-platform system is the subject of this research study that seeks to understand the importance of various modeling aspects on overall system performance.

## **1.2 Research Objectives and Methodology**

This research study is focused on three main objectives: (1) to develop the integrated 13.2 MW offshore wind turbine and semi-submersible platform model; (2) to compute and understand hydrodynamic forces on the platform

under expected wave loading; and (3) to investigate the system steady-state response due to wave loading as well as the system stochastic response under combinations of wind and wave loading. A summary of the tasks undertaken in this study is presented below.

### **1.2.1 Model Development for the Floating Offshore Wind Turbine**

The behavior of the land-based 13.2 MW wind turbine is studied so as to understand its steady-state response to uniform wind. This response to uniform winds is used to modify control parameters for the offshore wind turbine. The semi-submersible floating platform in this study is modeled based on the OC4 semi-submersible platform, with appropriate model scaling to support the larger 13.2 MW wind turbine. A mooring system is also developed for the overall wind turbine system.

### **1.2.2 Semi-submersible Platform Hydrodynamics**

To understand the semi-submersible platform hydrodynamics, the impact of wave loads on the platform is studied. Hydrodynamic effects on the platform include the combined effects of wave radiation, wave diffraction, hydrostatics, and additional inertial and drag loads on the different members of the platform. Linear hydrodynamics are considered in dealing with the problems of wave radiation and wave diffraction; potential flow theory is used in related analyses. The hydrostatics problem deals with stability in buoyancy and computations are based on the water-plane area. Additional



inertial and drag loads computed using strip theory or Morison's equation account for nonlinear hydrodynamics.

### **1.2.3 Steady-state and Stochastic Responses of the Integrated Turbine-Platform-Mooring System**

We first perform simulations under regular waves and in the absence of wind loading in steady-state response analyses in order to understand the dynamic behavior of platform. This steady-state response study is based on analyzing the periodic response due to unit-amplitude waves of different frequencies. We also assess the integrated system response under the influence of turbulent winds and irregular waves in order to understand the behavior of the turbine, platform, and mooring system under realistic environmental loading.

## **1.3 Limitations**

While we seek in this study to develop a model for the accurate prediction of the behavior of the integrated 13.2 MW wind turbine system, we wish to mention some limitations of our study.

We assume a specific size for the semi-submersible floating platform based on an assumption of adequate stability for the overall system; refinements in the sizing of the platform are certainly possible. We also assume that selected wind turbine control characteristics are appropriate for the offshore environment; parameters for this control system have been

adapted from those for the NREL 5 MW baseline offshore wind turbine supported by a semi-submersible platform. In all our hydrodynamic simulations, the wave heading is assumed in a direction aligned with the platform's positive  $x$ -axis (defined later) and along a line of symmetry for the platform. Thus, the hydrodynamics for this platform are studied for only this one wave heading. Accuracy of the linear hydrodynamics computations depends on the size and type of mesh employed to describe the platform surfaces; some refinements on the platform model in this regard are still possible. A major limitation on the model developed has to do with the lack of any available wave tank test data to allow any validation. Nonlinear hydrodynamic parameters are assumed to follow those employed in the OC4 system. A detailed analysis of the selected mooring system is not undertaken in this study.

One should interpret the results from this study in light of the above limitations. Additional research may be needed to address the influence of these limitations; in particular, additional model refinements may need to be made to obtain the desired performance of the overall turbine-platform-mooring system under realistic wind and wave loading.

## **1.4 Organization of Thesis**

Chapter 1 provided a general introduction to the problem studied, objectives of the study, and limitations. Chapter 2 describes floating wind turbine concepts in general, simulation tools used in this study, and the

development of the integrated system incorporating the 13.2 MW wind turbine, a semi-submersible platform, and a mooring system. Chapter 3 describes the theoretical framework and procedure used to define hydrodynamic loading on the platform. This chapter also explains the use of modeling and hydrodynamic analysis tools. Chapter 4 describes important modeling considerations in dynamic response simulation of the integrated turbine-platform-mooring system. We discuss the response of the floating platform to regular wave loading as well as the response of the integrated turbine system to irregular waves and turbulent wind fields. Finally, in Chapter 5, we summarize conclusions from this research study and offer some suggestions for future related research.

## Chapter 2

# Model Development for a Floating Offshore Wind Turbine

The development of deepwater floating offshore wind turbines is gaining interest in the renewable energy industry. While offshore wind energy development has been growing in Europe, only recently has there been increasing interest in studies related to bottom-supported and floating offshore wind turbines in the United States. Researchers at Sandia National Laboratories have recently developed a very large wind turbine model with 100-meter blades; such a large turbine is best suited for the offshore environment and will possibly be deployed in deep waters. It is a challenge to develop a model for a floating offshore platform that must provide support and stability to a large wind turbine. Stability of the system at sea is important to maintain platform motions within acceptable limits. We choose a semi-submersible platform as the support structure that will be used to support the 13.2 MW wind turbine with 100-meter blades. This platform is composed of several members including three offset columns at each corner of a triangular hull that are connected by pontoons and cross frames to a main column above which the wind turbine is mounted. A semi-submersible platform is classified as buoyancy-stabilized due to the fact that it relies on

water plane area to achieve stability. A large water plane area allows the platform to resist larger wave-induced motions. The selected semi-submersible platform is also designed with base columns that act as heave plates for increased hydrodynamic damping in heave which in turn also reduces wave-induced motion in the vertical direction. These heave plates of the platform are important for stability of the overall system.

The wind turbine system is composed of three main models: the wind turbine, the semi-submersible platform, and a mooring system. Properties and specifications of these three models are presented in following sections. The simulation tools used for the offshore wind turbine and some details related to the development of the platform model are also presented.

## **2.1 Floating Wind Turbine Concepts**

The design of offshore wind turbines is challenging due to the need to consider the combined effects of aerodynamic and hydrodynamic loading. Floating wind turbines are best suited for deepwater sites whereas bottom-supported offshore wind turbines are preferred in shallow waters. The motions and loads for a floating offshore wind turbine are complicated due to the presence of wave-induced hydrodynamic loads (diffraction), platform-induced hydrodynamic loads (radiation), some coupled motions between the wind turbine's rotor-nacelle assembly and the supporting floating platform, and the dynamic characteristics of the mooring system. Additional considerations relate to the impact of marine growth and possible

impact of floating debris or sea ice. Several floating platform configurations used in the oil and gas industry can also be considered for supporting an offshore wind turbine. These are separated into three classes depending on the different combinations of mooring systems, tanks, and ballasts that are part of the design [3, 6, 13]. The three classes of floating wind turbine concepts classified based on how they provide stability are illustrated in Figure 2.1 and described as follows:

- **Ballast-stabilized:** These designs rely on a deep draft and heavy ballast to provide hydrostatic stability. The center of buoyancy is designed so as to always lie above the platform's center of gravity. Thus, the buoyancy force resists motions in roll and pitch. A spar buoy is an example of a ballast-stabilized floating platform. It experiences very small effects due to wave radiation and diffraction but ballasting of slender cylindrical spars requires a lot of material which increases associated costs.
- **Mooring-stabilized:** These designs rely on tensioned mooring lines to hold the platform below the mean sea water level and resist motions in heave and pitch. The tension leg platform (TLP) is an example of a mooring-stabilized floating platform. Such platforms are considered costly due to materials but especially due to the high-tensioned mooring system required.
- **Buoyancy-stabilized:** These designs rely on the water plane area moment of the platform to achieve stability. Example of platforms

designed on this concept include barges (shallow-drafted rectangular or circular platforms) and semi-submersible platforms (usually with three or four offset columns connected together). Stability is achieved by raising the metacenter point above the centers of gravity and buoyancy of the platform. As the water plane area of a buoyancy-stabilized platform increases, it becomes less susceptible to wave-induced loadings.

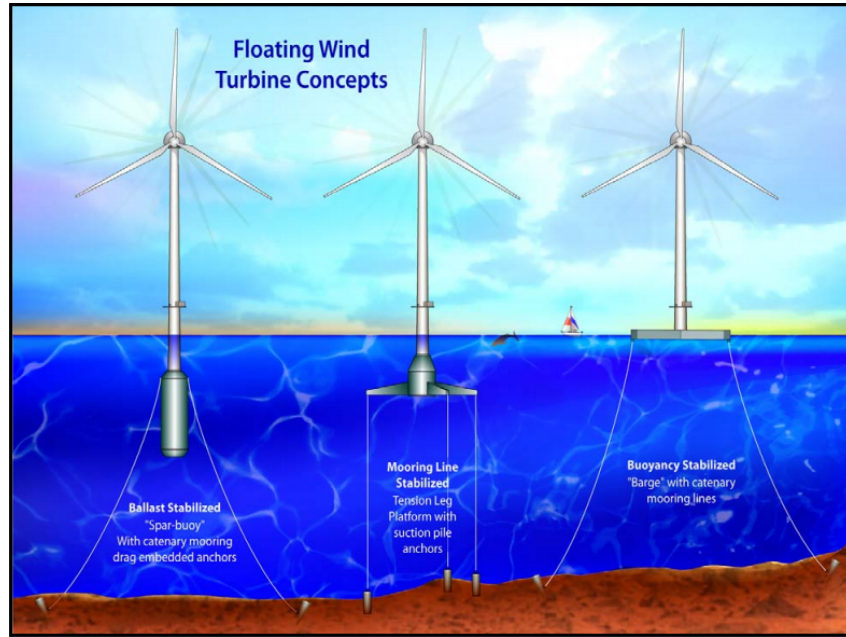


Figure 2.1: Floating offshore wind turbine concepts classified based upon how they provide stability [3].

## 2.2 Simulation Tools for Model Development

To make it possible to carry out response analyses of the integrated turbine, platform, and mooring system, simulation tools are needed to represent the aerodynamic model, platform hydrodynamics, and the mooring lines. FAST is the main simulation tool that combines these three separate parts; the newest version of FAST (version 8) is modularized for efficiency compared to older versions [14–16]. FAST requires inflow wind velocity fields that are simulated over the rotor plane of the wind turbine using TurbSIM [17, 18]. Model development and hydrodynamic analysis for the platform requires the use of MultiSurf [19] and WAMIT [8]. Hydrodynamic parameters and forces, computed by WAMIT, are used in FAST to couple with the wind turbine aerodynamics module. Analysis of the mooring system is introduced using the MAP module [7]. A summary of the design and simulation tools along with the various modules needed in an overall system response analysis is presented in Figure 2.2.



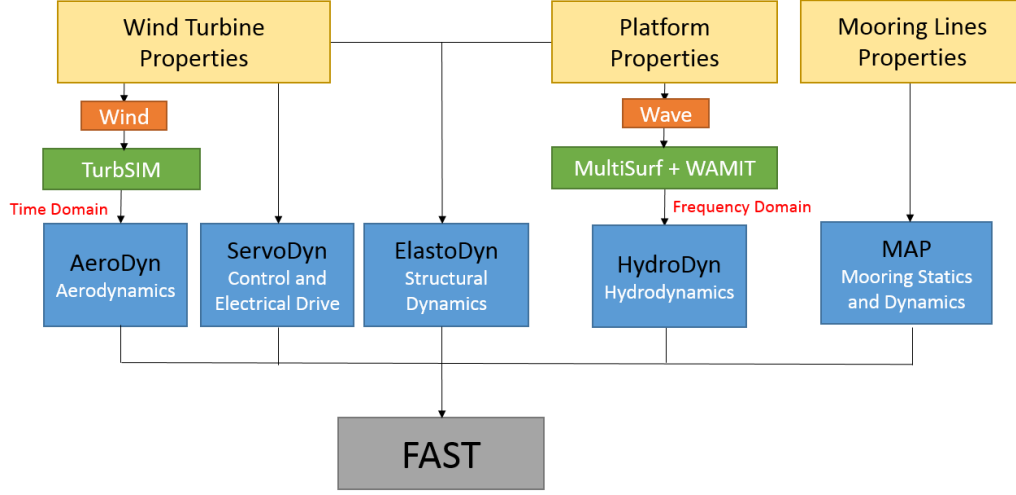


Figure 2.2: Simulation tools and modules for the integrated turbine, platform, and mooring system.

### 2.2.1 FAST

The open-source turbine system simulation tool, FAST (Fatigue, Aerodynamics, Structures, and Turbulence), was developed by researchers at the National Renewable Energy Laboratory (NREL) [14–16]. FAST is a fully coupled dynamic analysis program that is used for onshore and offshore wind turbine simulations. A wind turbine mounted on a floating semi-submersible offshore platform is the focus of this study. For wind turbines supported on floating platforms, FAST includes three components: the wind turbine, the floating platform, and a mooring line system. The various modules involved in a FAST analysis include AeroDyn, ServoDyn, ElastoDyn, HydroDyn, and MAP (see Figure 2.2). In the AeroDyn module, both steady and unsteady inflow wind fields generated by TurbSIM in the time domain are used to

compute aerodynamic loads on the rotor; tower drag loads are also computed in this module. The electrical drive system and control system for the wind turbine are inputs to ServoDyn. In ServoDyn, the blade-pitch controller and the variable-speed controller, important for overall stability of the system, can be modified as needed. ElastoDyn deals with the overall structural dynamics of the entire system; a total of up to 23 degrees of freedom can be represented in ElastoDyn. Six of these degrees of freedom correspond to translational and rotational motions of the floating platform. The tower is modeled as a flexible body; the first two modes of vibration in the fore-aft and side-to-side directions are included as degrees of freedom. Similarly, the flexible blades provide nine additional degrees of freedom resulting from nine modes of vibration for the three-bladed turbine model—two each in flap-wise bending and one in edge-wise bending for each blade. In version 8 of FAST, the furling degree of freedom is neglected. Hence, the remaining four degrees of freedom include rotor teeter, generator azimuth, drivetrain torsion, and nacelle yaw. The HydroDyn module takes into consideration first- and second-order hydrodynamics. Morison’s equation is used for the structural members of the platform; different hydrodynamic coefficients can be input for each member in this module. Ballasting of the platform is also accounted for in HydroDyn. The mooring line system response analysis is based on a quasi-static approach using the MAP module.

### 2.2.2 TurbSIM

TurbSIM program is a simulator used for generating inflow turbulent wind field on a rectangular grid defined over the rotor plane of the wind turbine [17, 18]. Zero-mean turbulence for three orthogonal components is simulated in the time domain at each grid point; a specified average hub-height wind speed and associated wind shear profile are added to the simulated longitudinal component of turbulence. A Kaimal power spectral density function (IECKai) is assumed to generate the turbulence components in the three orthogonal directions. The turbulence intensity ( $I_{ref}$ ) (corresponding to a hub-height wind speed of 15 m/s) is assumed to be 0.14; this corresponds to turbulence category ‘B’ according to IEC 61400-1 [20].

### 2.2.3 WAMIT

WAMIT [8], developed by WAMIT Inc. and the Massachusetts Institute of Technology, is a linear hydrodynamics solver which uses potential flow theory and integrates pressures by the panel method to yield a converged solution of the diffraction and radiation problems on the body surface for a specified mode, wave frequency, and wave heading. The hydrodynamic parameters obtained from a WAMIT analysis are used as input to the HydroDyn module in FAST. Two output files from WAMIT, the *Model.1* file that contains added mass and damping coefficients and the *Model.3* file with wave excitation forces, are specifically needed. The hydrostatics file (*Model.hst*) contains the hydrostatic restoring coefficients

and provides another input to FAST.

#### 2.2.4 MultiSurf

MultiSurf [19], developed by AeroHydro Inc., is a computer-aided design (CAD) program that is used to build a model of the floating platform. A body surface mesh is created in this program in order to evaluate forces on the platform from wave-induced and platform-induced motions. MultiSurf is also used to create other WAMIT input files that describe wave characteristics and platform dimensions (these include *Model.gdf*, *Model.pot*, *Model.cfg*, and *Model.frc*). The desired hydrodynamic analysis solvers are also specified (see Section 3.4); these solvers for WAMIT are described in Section 3.3.

### 2.3 SNL 13.2 MW Wind Turbine Model

Wind turbines with very large rotors are being considered nowadays because of the expected lower cost of energy produced per unit. The Sandia National Laboratories' 13.2 MW wind turbine has 100-meter blades which are significantly longer than the longest blades being used today [12]. Figure 2.3 shows different currently used and proposed blades where the focus is on their lengths. For the 13.2 MW turbine, the turbine and tower dimensions were scaled up from the NREL 5 MW wind turbine [5, 21]. The hub height of this turbine is 146 m and the rotor diameter is 205 m. The rated wind speed for this machine is 11.3 m/s; the rated rotor speed is 7.44 rpm. Additional

properties of the turbine are listed in Table 2.1. These properties are based on the SNL 100-00 model [21, 22], which was further refined mainly to reduce its weight. Several parameters and configurations of this large wind turbine need to be carefully investigated to understand its behavior at offshore sites. The first stage in understanding the 13.2 MW wind turbine model is to study its behavior on land; the response of the land-based 13.2 MW wind turbine is the subject of a separate study [23].

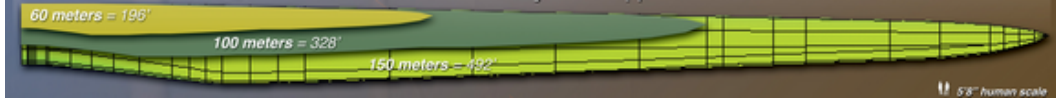


Figure 2.3: Currently used and proposed blade lengths [4].

Table 2.1: Properties of the 13.2 MW baseline turbine model.

Parameter	Value
Rated Generator Power	13.2 MW
Rotor Orientation, Configuration	Upwind, 3 Blades
Rotor, Hub Diameter	205 m, 5 m
Hub Height	146 m
Cut-In, Rated, Cut-Out Wind Speed	3 m/s, 11.3 m/s, 25 m/s
Rated Tip Speed	80 m/s
Cut-in, Rated Rotor Speed	4.34 rpm, 7.44 rpm
Generator Efficiency	94.4%
Overhang, Shaft Tilt, Precone	8.16 m, 5 degree, 2.5 degree
Tower Mass	1,532,937 kg
CM Location of Tower	63.7 m
Tower Damping Ratio	1%

Models for the 100-m blades have been refined to improve performance and to reduce weight and cost. Three versions of the blade have been proposed that are designed with the same external geometric dimensions but made of different materials. The first blade model developed was SNL 100-00, an all-glass baseline 100-meter wind turbine blade [5] with a weight of 114 tons. The second model developed was SNL 100-01, a carbon spar blade [24] with a weight reduction of 35% relative to SNL 100-00. Finally, a third blade model, SNL 100-02, was developed with advanced core material, modified from SNL 100-01 and with a weight reduction of 48% relative to SNL 100-00 and a 20% relative to SNL 100-01. Table 2.2 summarizes the main differences between the three blade models.

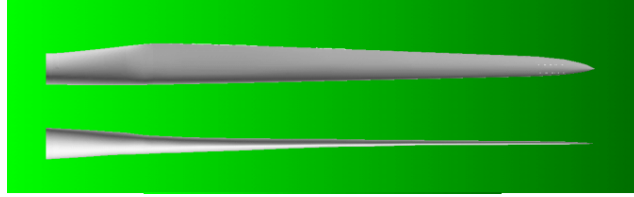
Table 2.2: Properties of the three 100-meter blade models.

Parameter	Value		
Blade Designation	SNL100-00	SNL100-01	SNL100-02
Blade Weight (kg)	114,172	73,995	59,047
Span-wise CG Location (m)	33.6	33.1	31.95
Lowest fixed-base natural frequency (Hz)	0.42	0.49	0.55
Blade Damping Ratio	0.477%	1.5%	1.5%

### 2.3.1 Blade Structural Properties

We discuss here the structural properties of the blades of the 13.2 MW wind turbine including the variation of their geometry, mass density, and stiffness over the length. Figure 2.4 shows flapwise, edgewise,

and isometric views of a blade. Figure 2.5 shows the variation of the blade mass density, flapwise stiffness, and edgewise stiffness along the length of the blade. It can be seen that the SNL 100-00 blade (designated as Blade-00) has the highest mass per unit length and edgewise stiffness. Flapwise stiffnesses of all the blades are almost the same except near the blade root. The SNL 100-02 blade (Blade-02), with the lowest weight, is selected in the present study for model development of the coupled system of the turbine with the platform and mooring system. Figure 2.6 shows the flap and edge mode shapes for the three different blades; the mode shapes, assuming that the blade is fixed at its root, are very similar for all the blade models.



(a) Flap-wise and Edge-wise of the blade surface geometry



(b) Isometric of the blade surface geometry

Figure 2.4: Three views of the blade surface geometry: flapwise, edgewise, and isometric [5].

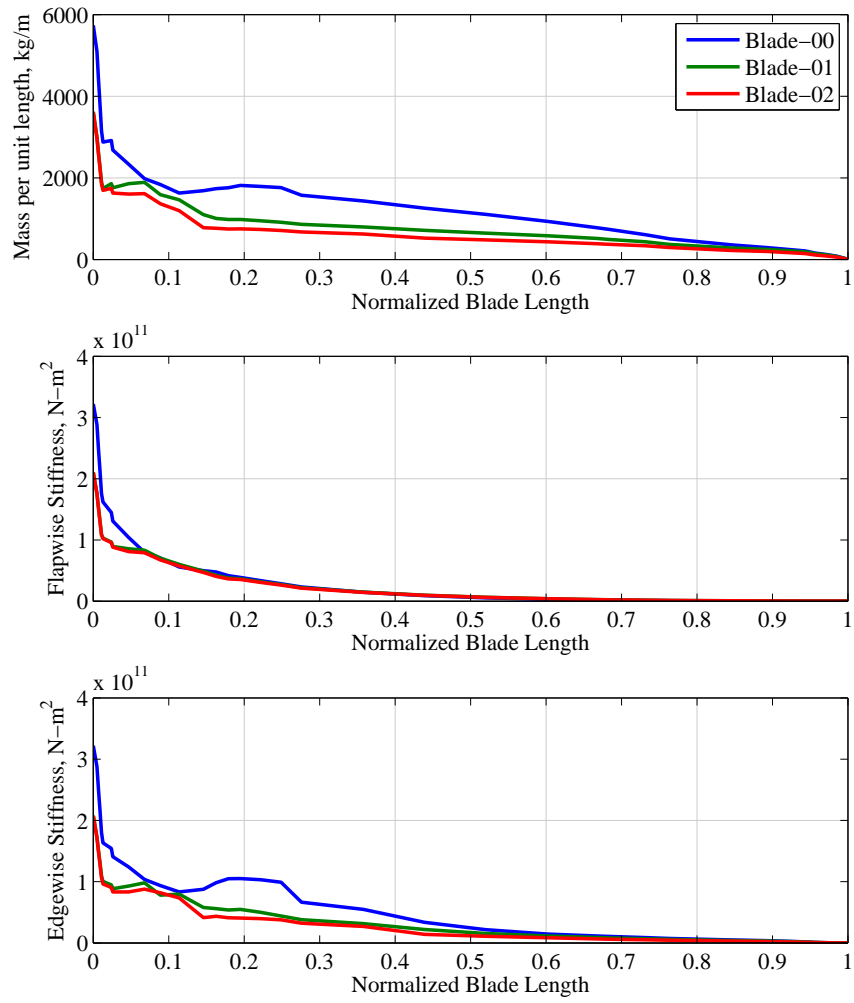


Figure 2.5: Variation in mass density, flapwise stiffness, and edgewise stiffness along the length for the three 100-meter blades.



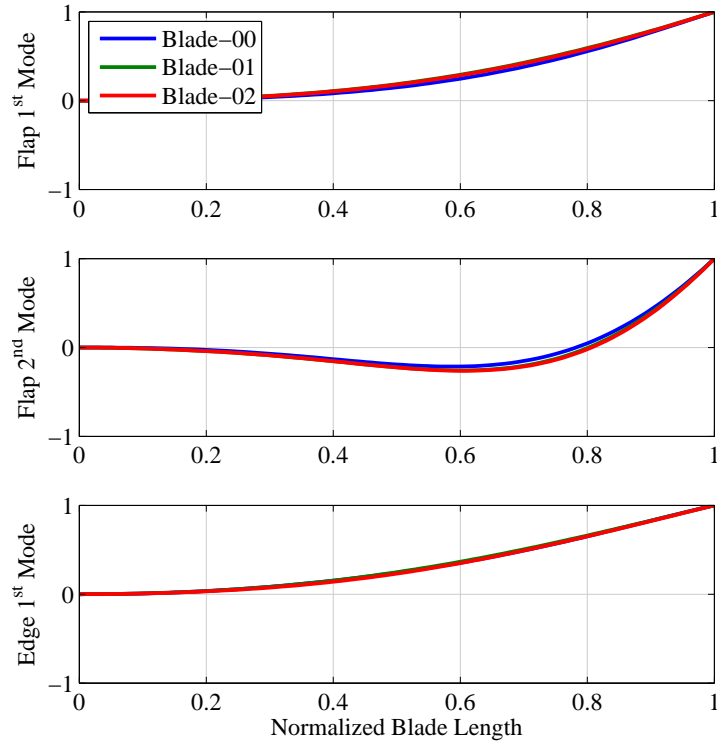


Figure 2.6: Flapwise and edgewise mode shapes for the three 100-meter blades.

### 2.3.2 Tower Structural Properties

The tower used for the 13.2 MW wind turbine was developed by researchers at Sandia National Laboratories; it is scaled up from the NREL 5 MW wind turbine tower [5]. This tower has a hub height of 146 m. The mass density and stiffness of the tower for the 13.2 MW turbine are scaled up by factors of 2.6471 and 7.007, respectively; their variation along the height of the tower is shown in Figure 2.7. The tower is symmetric about the fore-aft and side-to-side directions; hence, the fore-aft and side-to-side stiffnesses are identical. Figure 2.8 shows the first two mode shapes for

fore-aft and side-to-side bending of the tower, assuming a fixed base. The tower mass is 1,532,937 kg, while its center of mass is at 63.7 m from the base; a damping ratio is 1 percent of critical is assumed for the tower.

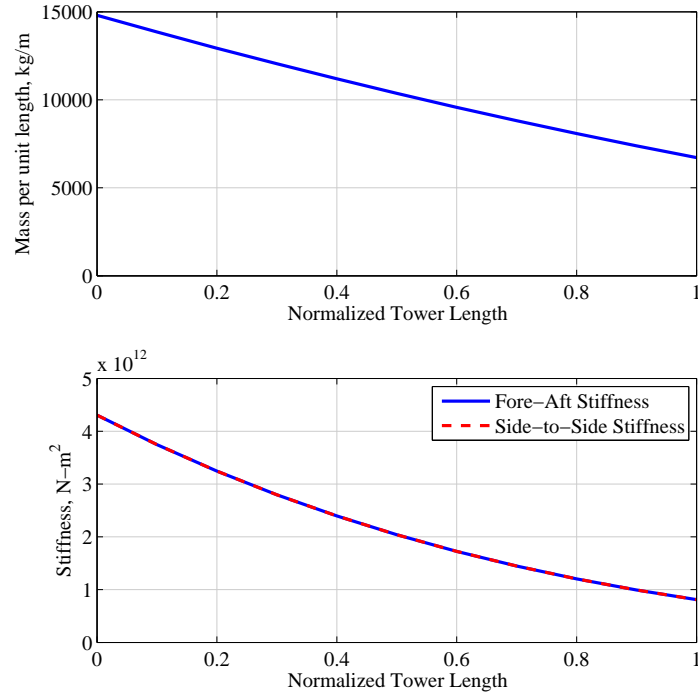


Figure 2.7: Variation of mass density and stiffnesses along the height of the tower.

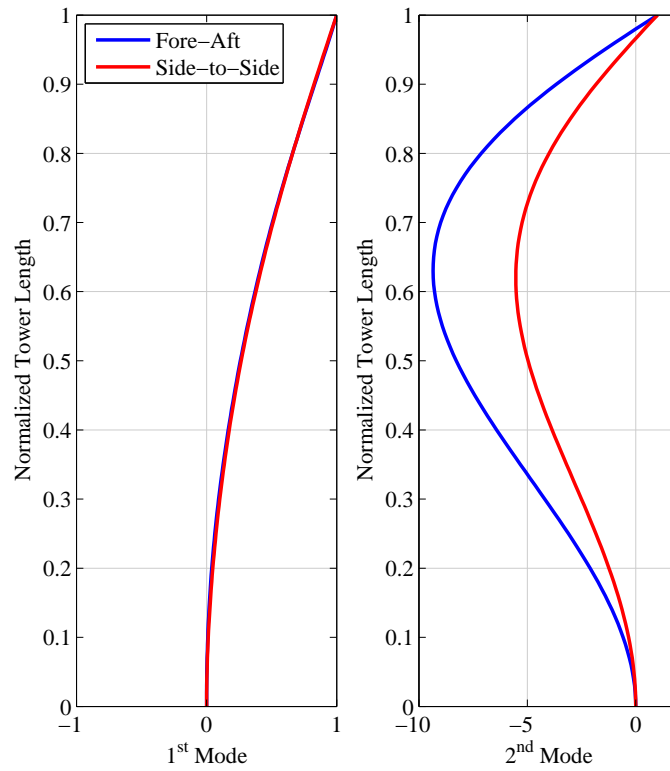


Figure 2.8: Fore-aft and side-to-side tower mode shapes.

### 2.3.3 Steady-State Response to Uniform Non-Turbulent Wind

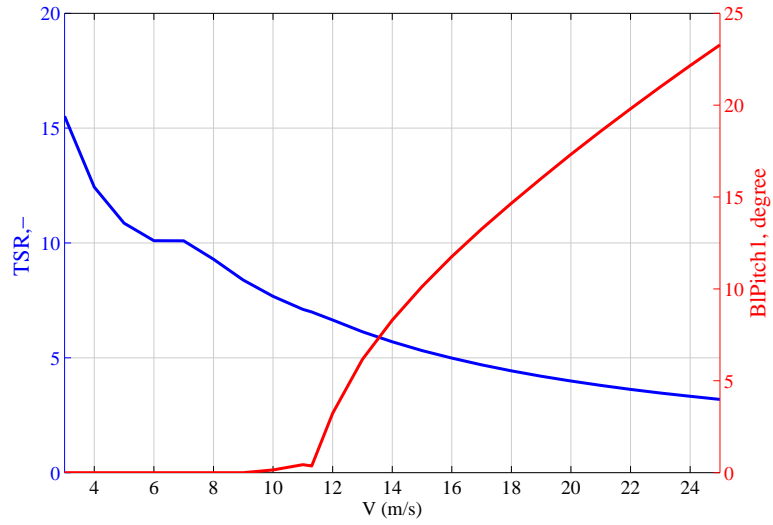
Figure 2.10 shows the steady state response of the 13.2 MW wind turbine as a function of the hub-height wind speed. The various response quantities studied are as follows:

- **TSR** represents the tip-speed ratio.
- **BlPitch1** represents the pitch angle of Blade 1.
- **GenPwr** and **RotPwr** represent the generator output power and the

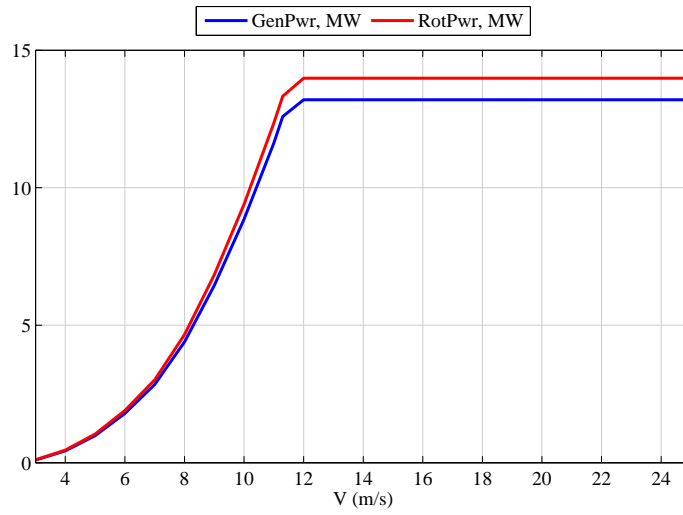
rotor input power.

- **GenSpeed** and **RotSpeed** represent the rotational speed of the generator and the rotor.
- **GenTq** represents the electrical torque of the generator.
- **RotTq** represents the rotor mechanical torque.
- **RotThrust** represents the rotor thrust.

We simulate a non-turbulent uniform wind field (with no shear) over the rotor plane and compute the steady-state response of the 13.2 MW land-based turbine using FAST. The response measures have contrasting characteristics over the regimes corresponding to below-rated, at or around rated, and above-rated wind speeds [3, 25]. Figure 2.9(a) shows that the blade pitch angle is held at zero below the rated wind speed; when the wind speed is above rated, the blade pitch angle increases continuously so as to lower loads on turbine and maintain rated power. From Figure 2.9(b), it can be seen that the rotor power is 13.98 MW, whereas the generator power is 13.2 MW; hence, the generator has an efficiency of 94.4%. From Figures 2.10(a) and 2.10(b), it is evident that the various response measures all increase with wind speed in the below-rated wind speed regime. When the rated wind speed is exceeded, the controller causes the blades to pitch to reduce thrust; constant rotor and generator torque and speed are maintained in order to produce constant power output.

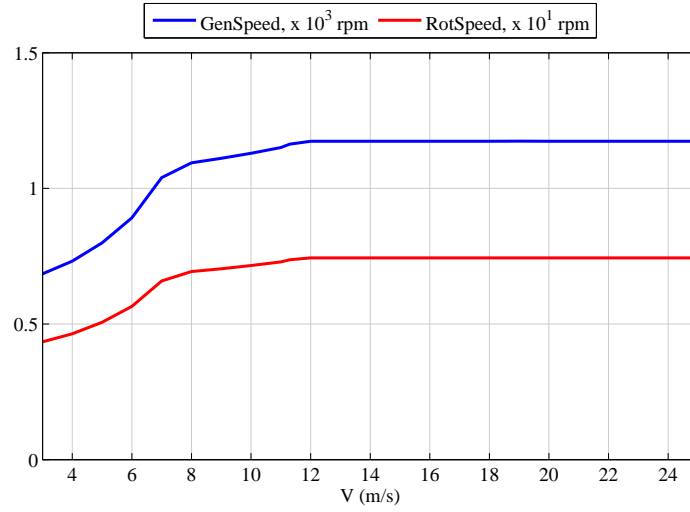


(a) Tip-Speed Ratio and Blade Pitch Angle.

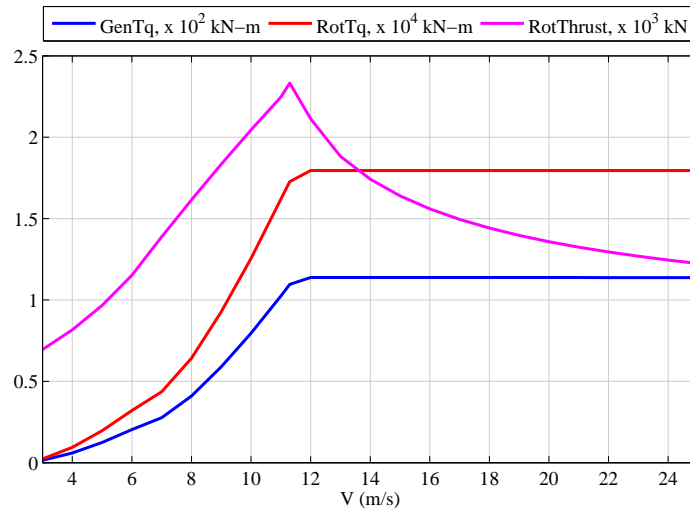


(b) Generator and Rotor Power.

Figure 2.9: Steady-state response of the 13.2 MW wind turbine as a function of hub-height wind speed: tip-speed ratio, blade pitch angle, generator power, and rotor power.



(a) Generator Speed and Rotor Speed.



(b) Generator Torque, Rotor Torque, and Rotor Thrust.

Figure 2.10: Steady-state response of the 13.2 MW wind turbine as a function of hub-height wind speed: generator speed, rotor speed, generator torque, rotor torque, and rotor thrust.

### 2.3.4 Control System for the 13.2 MW Offshore Wind Turbine

The controller for the 13.2 MW offshore wind turbine is adapted from the OC4 5 MW offshore wind turbine, with modifications in the blade pitch controller to prevent negative damping of the platform and in the variable-speed controller to adjust to the new turbine model [1, 26–28]. According to suggestions in OC3-Hywind [29] and OC4-DeepCwind studies, to avoid negative damping of the system, gains of the controller must be reduced in order to avoid resonant motions of the platform and to ensure that the blade pitching control frequency is below the dominant frequency of the system. An updated controller in the GH (Garrad Hassan) BLADED format was introduced in FAST in the form of a control system dynamic-link library file [16]. Table 2.3 summarizes the controller gains for the system.

The variable speed controller parameters were changed according to the 13.2 MW turbine specifications [5]. Because this turbine is very compared to the NREL 5 MW turbine, the maximum torque and power were modified to conform with Figures 2.9 and 2.10 above the rated wind speed. Table 2.4 summarizes variable speed controller parameters modified for the system.

Table 2.3: Blade pitch controller parameters employed in the OC4 project [1].

Parameter	Value
Integral gain at minimum blade-pitch setting ( $PC_{KI}$ )	0.000897
Proportional gain at minimum blade-pitch setting ( $PC_{KP}$ )	0.00628 s

Table 2.4: Variable speed controller parameters.

Parameter	Value
Maximum generator torque ( $VS_{MaxTq}$ )	115 kN-m/s
Maximum rated power ( $VS_{RtPwr}$ )	13.98 MW

## 2.4 Semisubmersible Platform

For the 13.2 MW wind turbine, which is significantly larger than its 5 MW counterpart, the semi-submersible platform model is developed by scaling up the OC4 semi-submersible platform by a factor of 1.8, based on consideration of the maximum tower base bending moment. This tower base bending moment is chosen as the basis for scaling because it effectively accounts for the overturning moment that needs to be resisted by the platform, when the turbine is mounted at an offshore site. The large water plane area of the platform provides a source of stability by introducing effective restoring inertias. The floating semi-submersible platform is designed to support the 13.2 MW wind turbine and limit platform motions due to winds and waves.

The platform model is scaled up from the OC4 DeepCwind semi-submersible platform design using a geometric scale factor,  $\lambda$ , equal to 1.8 [1]. Mass and moment of inertia are accordingly scaled by  $\lambda^3$  and  $\lambda^5$ , respectively, while the center of gravity is scaled by  $\lambda$ . The scaling law for platform properties and dimensions results from use of the Froude number and the turbine tip speed ratio (TSR) [2]. Wave tank tests for offshore



platforms utilize the Froude number to scale properties of a floating structure [30]; that same procedure is followed for the platform here. For a wind turbine, it is common to maintain the tip speed ratio (TSR) from the prototype to the scale model [2]. The scaling relationship adopted are summarized in Table 2.5.

The semi-submersible platform model is shown in Figure 2.11; structural and geometric properties of the platform are listed in Table 2.6. The wind turbine is mounted atop a main column. Three offset columns are connected together by a set of six pontoons between each column; the offset columns are also connected to the main column by a set of six pontoons and three cross-frame braces. The offset columns are 120 degrees apart. One offset column is assumed to lie along the negative  $x$ -axis while the other two offset columns are located symmetrically on either side of the positive  $x$ -axis. The platform is designed to experience limited heave motion by the introduction of a base column with a larger cylindrical diameter, beneath each offset column, that serves as a heave plate. The base of the wind turbine tower and the top of the main column of the platform are at an elevation of 18 meter above the still water level (SWL). The total draft of the platform extends 36 meters below the SWL.

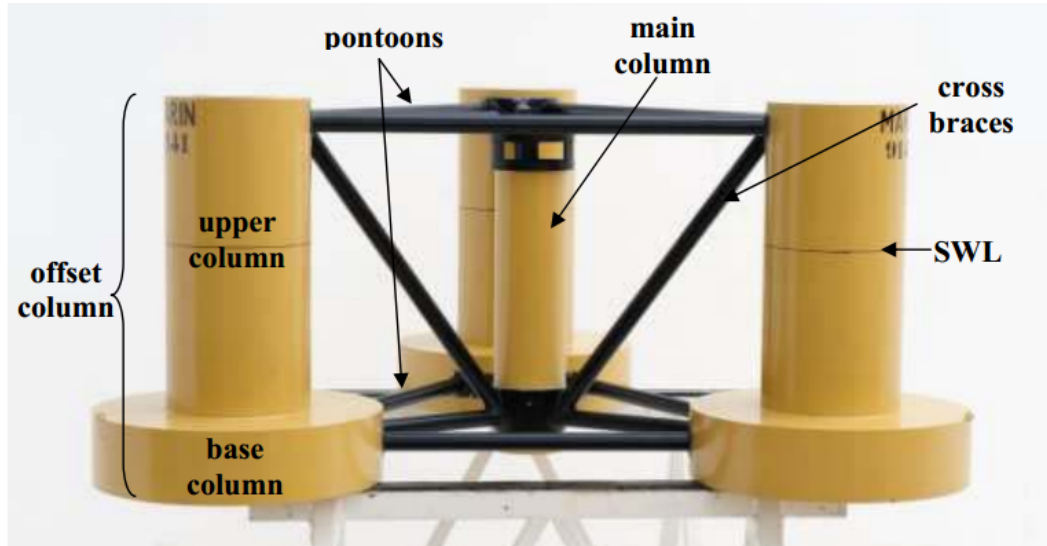


Figure 2.11: The semi-submersible platform model showing structural components [1].

Table 2.5: Scaling relationships for development of the platform model [2].

Parameter	Unit(s)	Scale Factor
Length	$L$	$\lambda$
Mass	$M$	$\lambda^3$
Mass moment of inertia	$ML^2$	$\lambda^5$

Table 2.6: Properties and dimensions of the semi-submersible platform.

Parameter	Value
Distance to platform base from SWL	36.00 m
Distance to top of main column from SWL	18.00 m
Distance to top of offset columns from SWL	21.60 m
Spacing between offset columns	90.00 m
Height of upper columns	46.80 m
Height of base columns	10.80 m
Diameter of main column	11.70 m
Diameter of upper columns	21.60 m
Diameter of base columns	43.20 m
Diameter of pontoons and cross braces	2.88 m
Platform mass including ballast without turbine	$7.86 \times 10^7$ kg
CG location below SWL	24.23 m
Platform roll inertia about CM	$1.28 \times 10^{11}$ kg-m <sup>2</sup>
Platform pitch inertia about CM	$1.28 \times 10^{11}$ kg-m <sup>2</sup>
Platform yaw inertia about CM	$2.25 \times 10^{11}$ kg-m <sup>2</sup>

#### 2.4.1 Platform Coordinate System

From an offshore wind turbine design perspective, the six degrees of freedom (DOFs) of the platform are translational motions of surge, sway, and heave along the  $x$ ,  $y$ , and  $z$  axes and rotational motions of roll, pitch, and yaw about the  $x$ ,  $y$ , and  $z$  axes. To geometrically describe the position and motion of the platform and wind turbine, a coordinate system is defined whose origin is defined at the floating platform's center where  $x = 0$  and  $y = 0$ . Also, the  $z = 0$  plane is selected at the still water level. Figure 2.12 shows the platform

coordinate system and the platform degrees of freedom. Motions in these six degrees of freedom are excited by waves on the platform. In this study, we only consider a single wave heading; both wind and waves are aligned and assumed to act in the positive  $x$  direction.

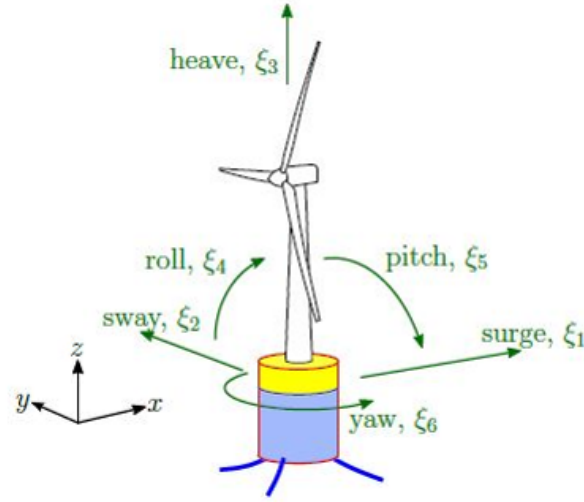


Figure 2.12: Reference coordinate system for the floating platform (illustrated for a barge platform) [6].

## 2.5 Catenary Mooring System

Mooring systems are important for floating offshore platforms because mooring lines limit the drift of a platform under wave and wind loading. For the floating semi-submersible platform supporting the 13.2 MW wind turbine, mooring lines of a catenary type are chosen. The mooring lines can be made from fiber rope, wire, and chain, or from some combination of the three. We assume a mooring system that is comprised of three catenary lines

connected to fairleads at the top of each base column of the platform. In Figure 2.13, the mooring line system is shown with the three mooring lines spread 120 degrees apart about the platform  $z$ -axis. One of the lines is directed along the negative  $x$ -axis; the other two lines are located symmetrically on opposite sides, 120 degrees apart from each other. The highest points of the mooring system in Figure 2.13 correspond to connections between the mooring lines and the fairleads at each base column at an elevation, 25.2 m below SWL. The mooring system is connected to the sea bed at anchor points; these anchor points are located at a water depth of 200 m below SWL and at a radial distance of 837.6 m from the platform center. The mooring lines are suspended from the fairleads and touch the sea bed with 309.6 meters of the individual lines lying along the sea floor. Properties of the mooring system are presented in Table 2.7. In future work, it may be useful to investigate alternative choices for the number and arrangement of mooring lines under specified performance constraints for the platform and wind turbine.

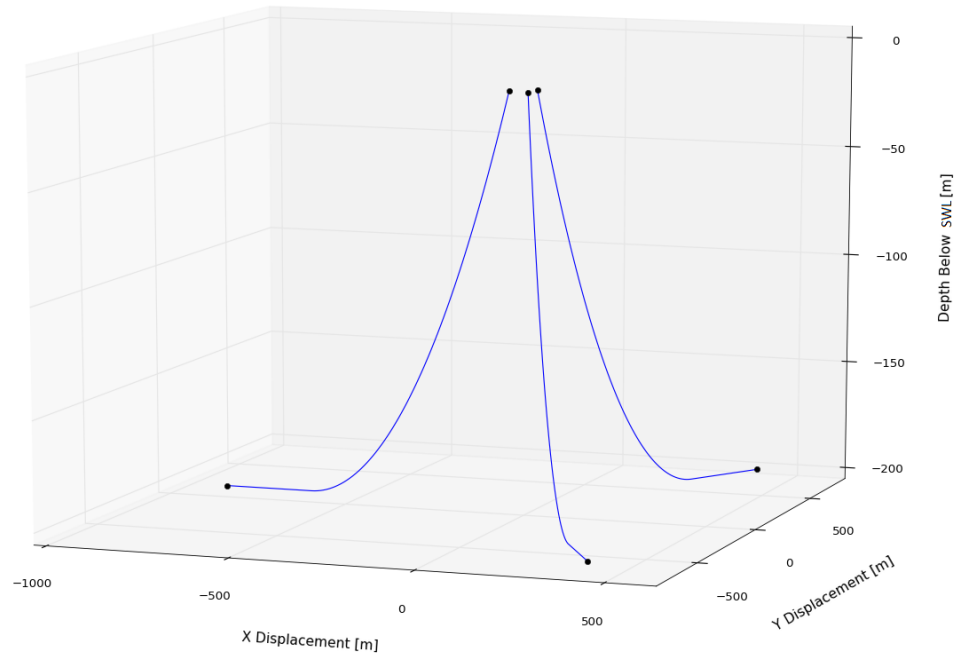


Figure 2.13: The catenary mooring line system for the semi-submersible platform [7].

Table 2.7: Mooring system properties.

<b>Parameter</b>	<b>Value</b>
Number of mooring lines	3
Angle between adjacent lines	120°
Depth to Anchors below SWL (Water Depth)	200 m
Depth to Fairleads below SWL	25.2 m
Radius to Anchors from Platform Centerline	837.6 m
Radius to Fairleads from Platform Centerline	73.56 m
Unstretched Mooring Line Length	835.5 m
Length of Mooring Line along Sea Bed	309.6 m
Mooring Line Diameter	0.13788 m
Equivalent Mooring Line Mass Density	367.25 kg/m
Equivalent Mooring Line Apparent Mass in Water	351.96 kg/m
Equivalent Mooring Line Extensional Stiffness	2442 MN
Seabed Drag Coefficient for Mooring Lines	1.0

# Chapter 3

## Semi-submersible Platform Model Hydrodynamics

In this chapter, we present procedures related to the linear hydrodynamic effects on the semi-submersible platform resulting from wave excitation from incident waves, the added mass component from the platform motions, and wave-radiation damping from the radiated wave outward from the surface of platform. The dynamic response analysis of a semisubmersible platform requires that, in addition to the linear hydrodynamic effects noted, both nonlinear damping effects due to hydrodynamic drag forces as well as inertia forces should be accounted for [31, 32]; these are discussed in Chapter 4. All the linear hydrodynamics contributions (added mass, damping, and wave excitation coefficients) are obtained using WAMIT.

The steps involved in obtaining the required hydrodynamic coefficients are indicated in Figure 3.1 and briefly described as follows:

- Establish the scale of the platform that is suitable to limit motions of the system and provide stability.
- Model and mesh a B-spline surface of the platform with appropriate panelization using MultiSurf.



- Generate WAMIT input files for the platform geometry and coordinates, wave characteristics, water depth, configuration for solvers, and required WAMIT hydrodynamics. The relevant input files are *Model.gdf*, *Model.pot*, *Model.cfg*, and *Model.frc*, respectively.
- Create a WAMIT input file that controls the output file names (*fnames.wam*).
- Create a WAMIT input file that specifies the path of the simulations and the number of processors and amount of memory (RAM) to be used for the analysis (*config.wam*).
- Simulate the platform in WAMIT using the “higher-order” solution approach (with B-spline mesh lines) using RGKERNEL, a direct solver, and remove the effect of irregular frequencies from the simulations.
- Post-process the hydrostatics (*Model.hst*) files and the linear hydrodynamics files (Added mass - *Model.1*, Damping - *Model.1*, and Wave excitation - *Model.3*) to be used as HydroDyn inputs [33] in FAST.

Inputs for HydroDyn are separated into those for the radiation, diffraction, and hydrostatics problems; WAMIT is well-suited to generate these using a potential flow theory solution. The waves that act as external force on the platform are described in Section 3.1. The theoretical basis for the hydrodynamic parameters derived from WAMIT is briefly discussed in

Section 3.2. Input files for WAMIT and modeling criteria for the floating platform are described in Sections 3.3 and 3.4. The added mass, damping, and wave excitation coefficients for the platform's six degrees of freedom are presented in Section 3.5.

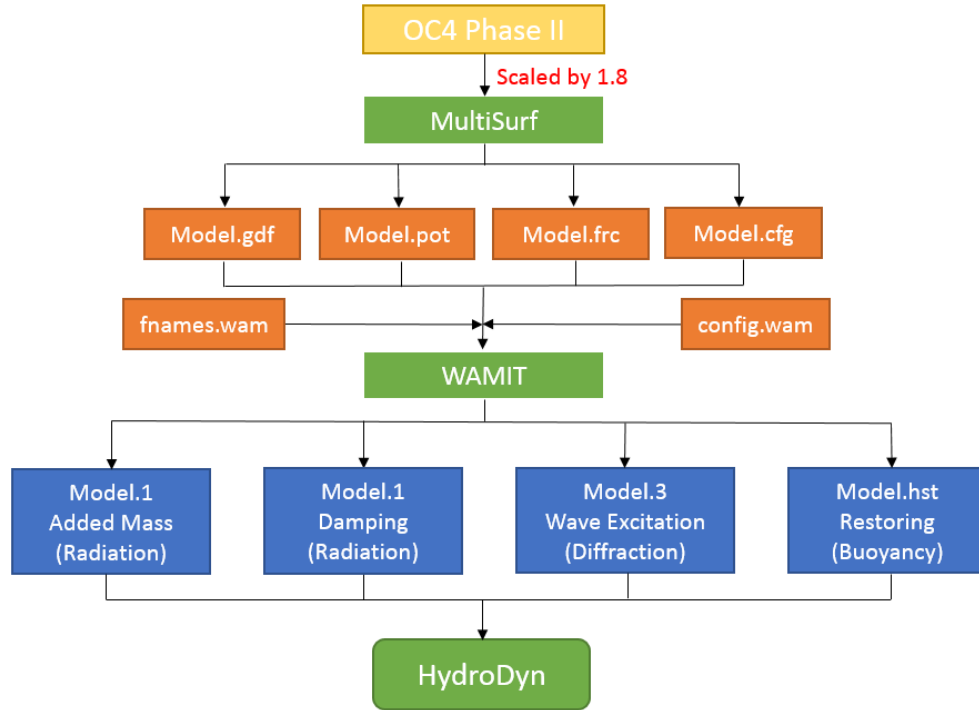


Figure 3.1: Flow chart for obtaining desired hydrodynamic coefficients (FAST inputs for the HydroDyn module).

### 3.1 Hydrodynamic Loading on the Floating Platform

Hydrodynamic loads on the platform result from three distinct components—platform motions that are part of the “radiation” problem; waves related to the “diffraction” problem; and buoyancy effects of the platform that are part of the “hydrostatics” problem. These different components are illustrated schematically in Figure 3.2.

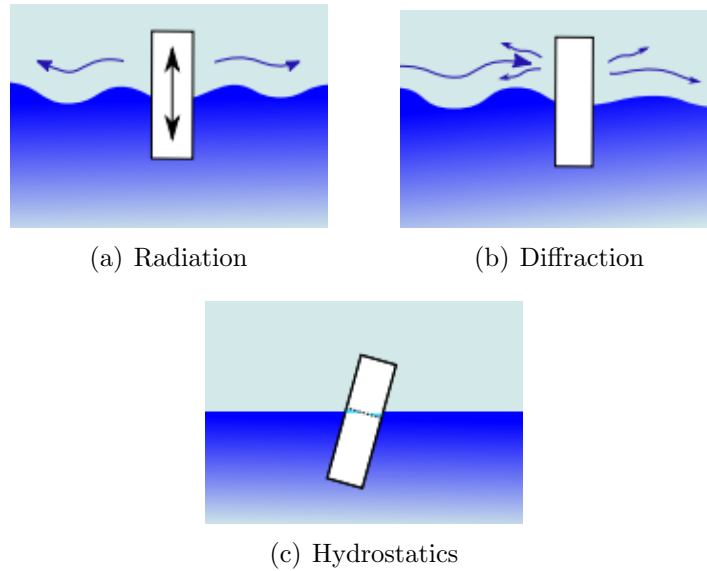


Figure 3.2: Linear hydrodynamic effects illustrated for a vertical cylinder [6].

**The radiation problem** is related to waves generated and radiated outward from the surface of the platform after platform motions from the incident waves have stopped. Two effects from the radiation problem are of importance; these are added-mass effects and wave-radiation damping. Added mass refers to the additional component of the mass of water that is

accelerated together with the platform when the platform moves. External forces on the platform from different wave frequencies will have different added mass coefficients. Forces due to added-mass effects are proportional to the platform acceleration. Wave-radiation damping resulting from the linear hydrodynamics analysis leads to reduced motion of the platform after the incident wave passes it. Waves radiate around the platform and cause the platform to oscillate. Derived damping coefficients are proportional to the platform velocity. Different wave frequencies lead to different damping coefficients as is the case with the frequency-dependent added-mass coefficients.

The relationship between hydrodynamic forces and the diameter of the platform may be understood by studying the Keulegan-Carpenter number,  $K_c$ , as follows [6, 13]:

$$K_c = \frac{VT}{D} \quad (3.1)$$

where  $V$  is the amplitude of the wave velocity,  $T$  is the period of oscillations, and  $D$  is a characteristic length scale of the platform or pile.

The following dispersion relationship for deep water relates the wavelength,  $L$ , to the wave period,  $T$ :

$$L = \frac{gT^2}{2\pi} \quad (3.2)$$

where  $g$  is the acceleration due to gravity.

When the platform dimensions are significantly larger than the wavelength,  $K_c$  is small and inertial forces dominate. Then, added-mass and

damping coefficients from linear wave theory provide good approximations for computing hydrodynamic forces on the platform. On the other hand, drag forces are dominant when  $K_c$  is large. For a large value of  $K_c$ , the ratio of the platform characteristic length to the wave period is small relative to the flow velocity; then, the wavelength is significantly large compared to the platform dimensions. For large  $K_c$  values, nonlinear hydrodynamic loads and additional viscous and inertia forces on multiple members, apart from the main body itself, need to be taken into consideration. For small  $K_c$  values, added-mass and damping coefficients derived using WAMIT are most important and are evaluated for all six degrees of freedom of the platform. Due to coupling between some of the degrees of freedom, these linear coefficient matrices have some non-zero off-diagonal terms. Six-by-six frequency-dependent matrices representing effects of added mass,  $\mathbf{A}_{ij}(\omega)$ , and wave-radiation damping,  $\mathbf{B}_{ij}(\omega)$ , are evaluated and related to linear hydrodynamic forces in the direction of degree-of-freedom (DOF),  $j$ , due to motion in DOF,  $i$ .

**The diffraction problem** is related to waves diffracted around the platform. When the platform stops to move from excitation by the incident wave, waves are scattered and diffracted. These effects are minimal when the wavelength is considerably larger than the dimensions of the platform [34]. In such cases, excitation forces can be evaluated based on the undisturbed wave kinematics alone [6]. Since the wave does not travel through the platform, no velocity potential flow exists through the surface. Wave excitation forces

and moments are calculated by integrating over the surface of the platform using Green’s theorem. Forces and moments from the wave excitation effect are calculated based on Laplace and Bernoulli equations in the potential flow theory of WAMIT [8]. Frequency-dependent excitation forces and moments  $\mathbf{X}_i(\omega, \beta)$  are generated for specified wave heading angles,  $\beta$ .

**The hydrostatics problem** is related to computation of the static restoring coefficients based on the water plane area at the undisplaced position of the platform, the displaced volume of water from the platform buoyancy, and the center of buoyancy. It accounts for the buoyancy of the platform when it is displaced in water. When waves excite the platform, self-stabilization is required under the combination of buoyancy forces, the weight of the system, and external forces and moments. Six-by-six frequency-independent matrices,  $\mathbf{C}_{ij}$ , are generated to define forces in the direction of DOF  $j$  from unit translation or rotation in DOF  $i$ . The water plane area affects hydrostatic coefficients in heave, roll, and pitch, while it has no effect on surge, sway, and yaw.

### 3.2 Analysis using WAMIT

WAMIT is a radiation and diffraction panel method program for linear hydrodynamic analysis to evaluate unsteady hydrodynamic loads and motions of a body in a fluid domain. Airy wave theory is used to describe first-order linear waves. WAMIT uses potential flow theory and Laplace’s equation with appropriated boundary conditions; linear hydrodynamic loads

are computed from the superposition of solutions of the radiation, diffraction, and hydrostatic problems, each of which follows Laplace's equation. With potential flow theory, the flow is defined as incompressible and irrotational.

Analysis using WAMIT yields four important inputs to FAST that include hydrostatic restoring, added mass, damping, and wave excitation coefficients. The incident wave excitation force is in complex form and depends on the wave heading direction,  $\beta$ . The equation of motion for the six degrees of freedom of the floating offshore platform for a harmonic wave input with amplitude,  $A_{wave}$ , and frequency,  $\omega$ , is given as follows:

$$(\mathbf{M}_{ij} + \mathbf{A}_{ij}(\omega)) \ddot{\xi}_j(t) + B_{ij}(\omega) \dot{\xi}_j(t) + \mathbf{C}_{ij} \xi_j(t) = A_{wave} \mathbf{X}_i(\omega, \beta) e^{i\omega t} \quad (3.3)$$

where

$\mathbf{M}_{ij} = 6 \times 6$  platform physical mass matrix;

$\mathbf{A}_{ij} = 6 \times 6$  added mass matrix;

$\mathbf{B}_{ij} = 6 \times 6$  damping matrix;

$\mathbf{C}_{ij} = 6 \times 6$  stiffness matrix;

$\mathbf{X}_i = 6 \times 1$  wave excitation vector;

$\xi_j(t) = 6 \times 1$  displacement or rotation vector;

$\dot{\xi}_j(t) = 6 \times 1$  vector of first derivatives of the displacement or rotation;

$\ddot{\xi}_j(t) = 6 \times 1$  vector of second derivatives of the displacement or rotation;

$A_{wave}$  is wave amplitude.

It is convenient to derive a solution for  $\xi_j(t)$  in terms of a complex

response function,  $\Xi(\omega)$ , as follows for any wave heading,  $\beta$ :

$$\xi_j(t) = \Xi(\omega)e^{i\omega t} \quad (3.4)$$

The equation of motion in the frequency domain can then be written as:

$$\left[ -\omega^2 (\mathbf{M}_{ij} + \mathbf{A}_{ij}(\omega)) + i\omega \mathbf{B}_{ij}(\omega) + \mathbf{C}_{ij} \right] \Xi(\omega) = A_{wave} \mathbf{X}_i(\omega, \beta) \quad (3.5)$$

It is convenient to define a Response Amplitude Operator,  $RAO_j(\omega)$ , which represents the response per unit wave amplitude. An  $RAO$  for any displacement or rotation, defined in this way, can represent the steady-state frequency response of a floating platform accounting for the effects of wave excitation, added mass, damping, and hydrostatic stiffness. This requires a regular wave analysis in WAMIT for a specified wave heading. The  $RAO$  can be defined as follows:

$$RAO_j(\omega) = \frac{\Xi(\omega)}{A_{wave}(\omega)} \quad (3.6)$$

where  $j$  corresponds to the degree of freedom (displacement or rotation) of the platform.

### 3.3 Use of WAMIT

WAMIT is a hydrodynamic analysis program which is based on potential flow theory and uses a panel method computational approach. Coefficient matrices and/or vectors defining the added mass, wave-radiation damping, and wave excitation forces result from the linear wave



hydrodynamics solution and are needed to relate wave force effects on the platform with the HydroDyn module in FAST. WAMIT requires several input files to carry out the hydrodynamic analysis; these input files are generated using MultiSurf. WAMIT includes two subprograms, POTEN and FORCE. Input files needed by these subprograms include a geometry file (*Model.gdf*), a control file for the POTEN subroutine (*Model.pot*), a control file for the FORCE subroutine (*Model.frc*), two configuration files (*Model.cfg* and *config.wam*), and a file to define output file names (*fnames.wam*). Four of the input files (*Model.gdf*, *Model.pot*, *Model.frc*, and *Model.cfg*) are generated using MultiSurf while the two *.wam* files are generated using text file. Figure 3.3 shows a flow chart of various files involved in a WAMIT analysis.

### 3.3.1 Model.gdf

*Model.gdf* is a geometry data file. The model geometry is developed in MultiSurf using B-spline approximations that allow for smoothness and continuity of the panel mesh on the surface of the platform.

### 3.3.2 Model.pot

*Model.pot* is a control file used to define input parameters to the POTEN subprogram in WAMIT. This file defines the water depth, radiation solver, diffraction solver, number of wave periods or frequencies, the list of wave periods or frequencies, and the list of wave headings to be analyzed.

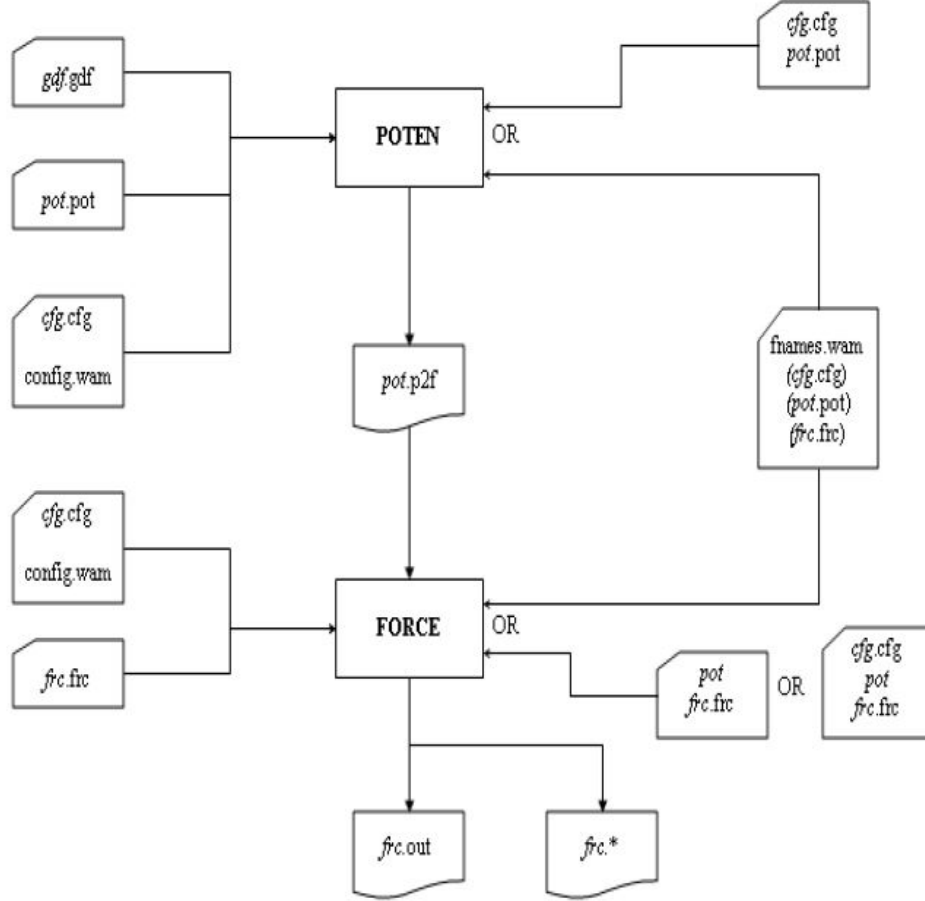


Figure 3.3: Flow chart showing various files involved in a WAMIT analysis [8].

The water depth,  $d$ , must be such that the following inequality is satisfied:

$$10^{-5} < d \times \frac{(2\pi f)^2}{g} < 10^5 \quad (3.7)$$

Given the water depth of 200 m, allowed incident wave frequencies can range from 0.00001 Hz to 11.1 Hz. The selected semi-submersible platform is

influenced more by waves in the low-frequency range than those in the high-frequency range; hence, WAMIT hydrodynamics solutions are evaluated for waves in the frequency range, 0 Hz to 0.7 Hz.

### 3.3.3 **Model.frc**

*Model.frc* is control file needed by the FORCE subprogram. Here, we specify that we are interested in added-mass and damping ( $A_{ij}$  and  $B_{ij}$ ) output to the file, *Model.1*. Likewise, wave excitation forces,  $X_i$ , are output to the file, *Model.3*.

### 3.3.4 **config.wam and Model.cfg**

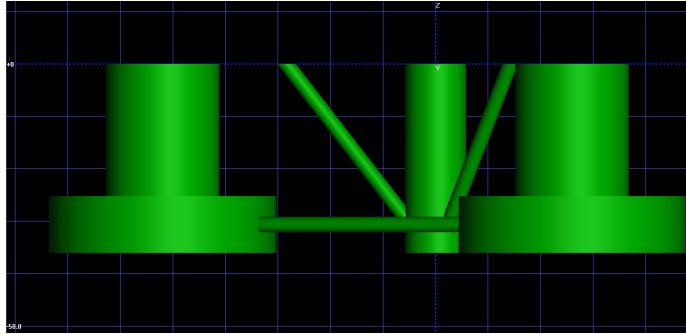
The two files, *config.wam* and *Model.cfg*, are configuration files. The file, *config.wam*, defines the path for the simulations, data storage, and the choice on processor(s). The file, *Model.cfg*, contains various other configuration parameters such as specifications of the use of a high-order method for surface geometry definition, the use of a direct solver, etc.

### 3.3.5 **fnames.wam**

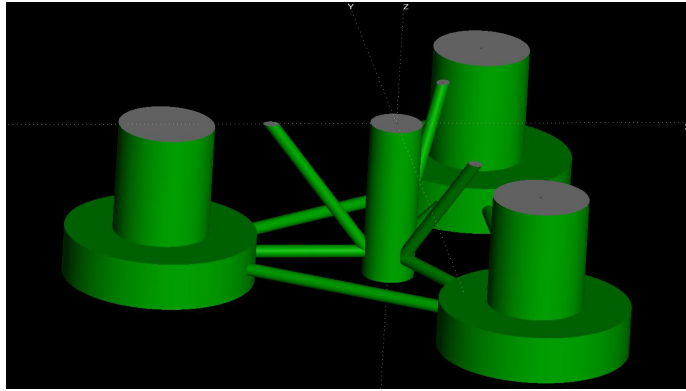
The file, *fnames.wam*, lists the names of the input filenames including *Model.gdf*, *Model.cfg*, *Model.pot*, and *Model.frc*. This file is used to automatically define the names of various output files (such as *Model.1*, *Model.3*, and *Model.hst*).

### 3.4 Use of MultiSurf

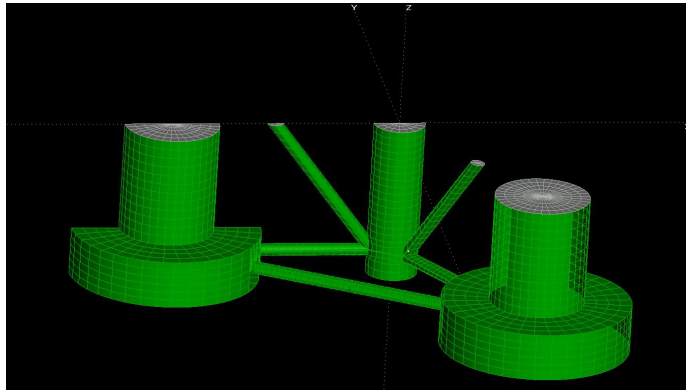
MultiSurf [19] is a 3D modeling tool that is useful for modeling a body such as a floating platform whose surface or shape may be difficult to create with other CAD packages. Also, MultiSurf has the ability to generate input files for WAMIT and one can import geometry files directly from MultiSurf models to directly use in WAMIT. The geometry of the semi-submersible platform is scaled up from the OC4 semi-submersible platform by a factor of 1.8. Modeling a platform in MultiSurf uses point, curve, and surface entities. These entities are used to create B-spline continuous curves to describe meshes and body geometry. A MultiSurf model of the platform is shown in Figures 3.4 and 3.5. Finer meshes are employed over parts of the platform to represent details around connections between members. To decide on the number of subdivisions to use in meshing, the area of each panel and processing time processing are important considerations. The typical size for a panel is 2 m. Taking advantage of symmetry about the  $x$ -axis, only model of the platform is developed and used in developing the platform model.



(a) Elevation XZ plane view of model below the SWL (Total draft is 36 m).

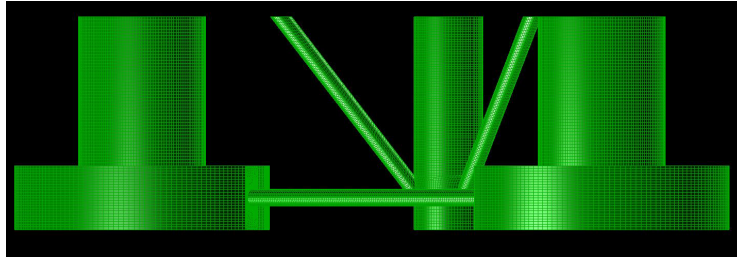


(b) Full model below the SWL.

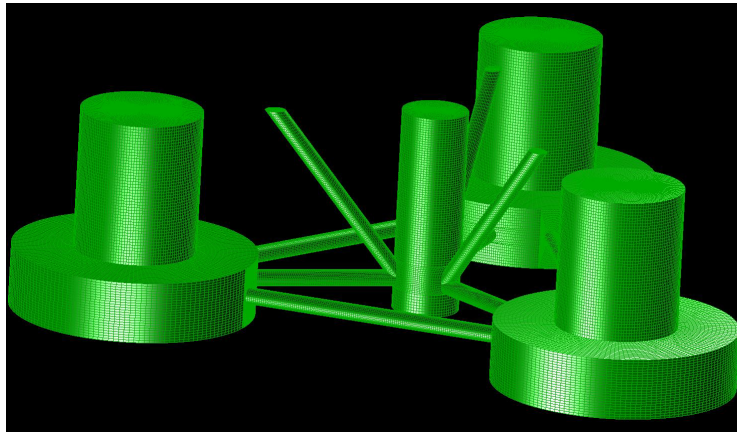


(c) Half model due to symmetry (cut along  $x$ -axis) shown with mesh.

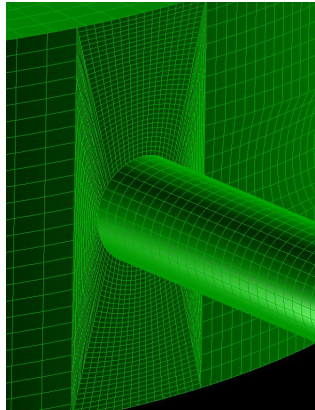
Figure 3.4: Different views of the MultiSurf model and mesh for the semi-submersible platform.



(a) Elevation XZ plane view of model below the SWL showing mesh.



(b) Full model below the SWL showing mesh.



(c) Mesh around a connection between a base column and pontoon.

Figure 3.5: MultiSurf models with division and subdivision meshes for the semisubmersible platform.

In an elevation XZ plane view of the model, the center of one offset column is located along the negative  $x$ -axis, 51.96 m radially from the platform center, whereas the other two offset columns are offset by 25.98 m in the direction of the  $x$ -axis (from the center) in that view. Grey portions of the model represent the still water level. The total number of panels is 53,760 including surface divisions and subdivisions. Table 3.1 shows the number of panels used for all the members of the semi-submersible platform model.

Table 3.1: Number of panels for the symmetric half model of the platform.

<b>Member</b>	<b>Number of Panels</b>
Main column	4,032
Half offset column	12,416
Full offset column	24,832
Pontoons and cross brace	12,480
<b>Total</b>	<b>53,760</b>

### 3.5 Linear Hydrodynamic Analysis Results from WAMIT

The hydrodynamic added-mass and damping coefficients and wave excitation forces are evaluated using WAMIT. For simulations in WAMIT, we consider a zero-degree wave heading (along the  $x$ -axis) and wave frequencies ranging from 0 to 0.7 Hz. Results from WAMIT analyses for the six DOFs are discussed next.

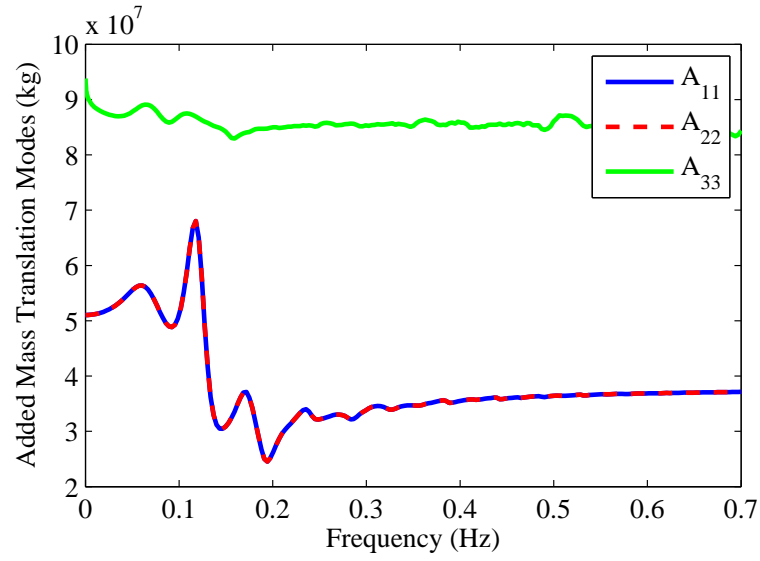
### 3.5.1 Added Mass

Figure 3.6 shows hydrodynamic added-mass coefficients for the three translational and three rotational DOFs (degrees of freedom) as a function of frequency. Figure 3.8(a) shows added-mass coefficients for coupled surge-pitch and sway-roll motions; these coefficients are identical but with opposite signs. At low wave excitation frequencies, added mass effects are larger, as can be seen in the figures. Added mass effects are quite low for wave frequencies much higher than 0.1 Hz since the wavelength in these cases is small relative to the platform dimensions (inertia forces are dominant). Due to platform symmetry, added mass coefficients in pure surge and sway modes are identical; similarly, those in pure roll and pitch modes are identical. Added-mass coefficient from coupled modes other than surge-pitch and sway-roll are zero. The added mass in heave is greater than that in surge and sway because the wetted surface and amount of displaced water from motions in heave is much larger than for surge and sway.

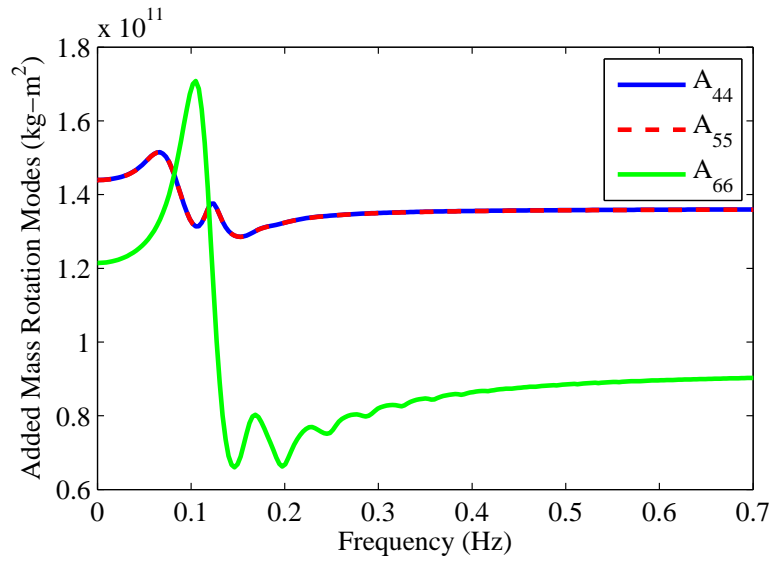
The added-mass matrix for infinite-frequency waves, needed in HydroDyn calculations, is as follows:

$$A_{\infty} = \begin{pmatrix} 5.1E7 \text{ kg} & 0 & 0 & 0 & -1.1E9 \text{ kg} \cdot \text{m} & 0 \\ 0 & 5.1E7 \text{ kg} & 0 & 1.1E9 \text{ kg} \cdot \text{m} & 0 & 0 \\ 0 & 0 & 8.7E7 \text{ kg} & 0 & 0 & 0 \\ 0 & 1.1E9 \text{ kg} \cdot \text{m} & 0 & 1.4E11 \text{ kg} \cdot \text{m}^2 & 0 & 0 \\ -1.1E9 \text{ kg} \cdot \text{m} & 0 & 0 & 0 & 1.4E11 \text{ kg} \cdot \text{m}^2 & 0 \\ 0 & 0 & 0 & 0 & 0 & 1.2E11 \text{ kg} \cdot \text{m}^2 \end{pmatrix}$$





(a) Added mass coefficients for translational motions.

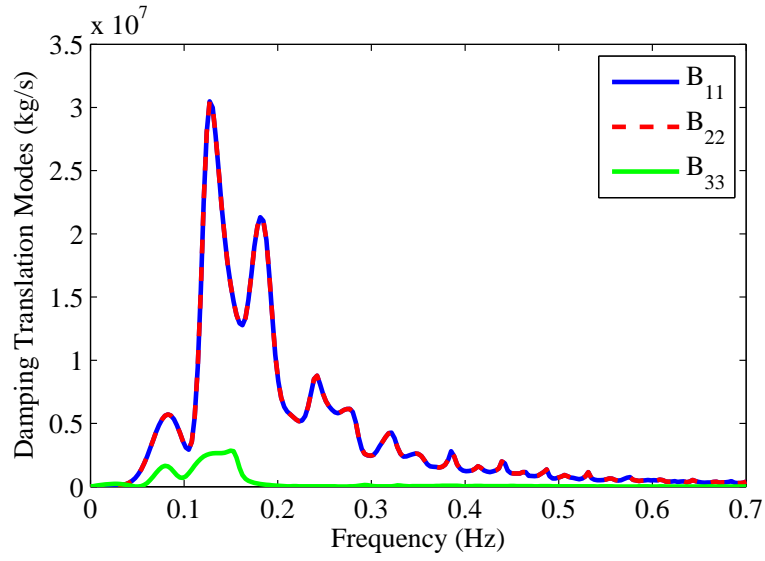


(b) Added mass coefficients for rotational motions.

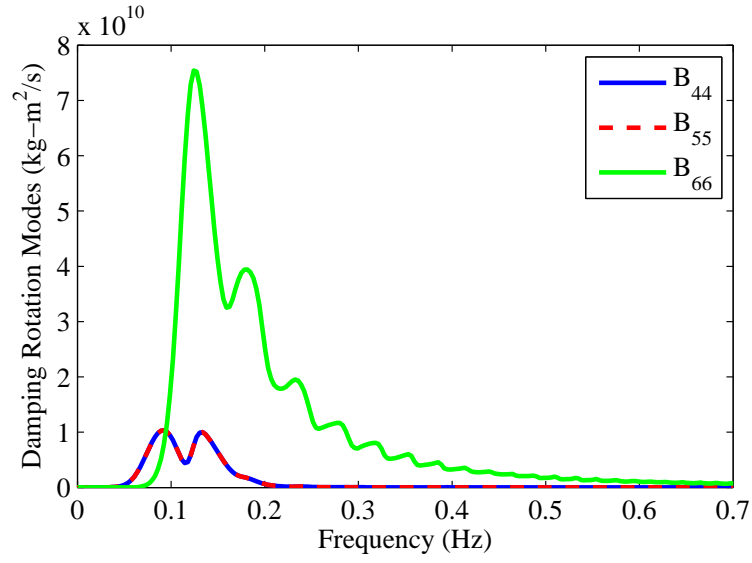
Figure 3.6: Added mass coefficients for the six degrees of freedom of the semi-submersible platform.

### 3.5.2 Radiation Damping

Hydrodynamic damping coefficients obtained from WAMIT analyses are presented in Figure 3.7 for the six degrees of freedoms as functions of frequency. Figure 3.8(b) shows damping coefficients for coupled surge-pitch and sway-roll motions; these coefficients are identical but with opposite signs. At very low as well as very high frequencies, the damping coefficients are almost zero. It is known too that the damping coefficient goes to zero when the wave frequency goes to zero for a circular cylinder [35]. For all six degrees of freedom, this platform has significant damping for waves in the 5-10 second period range; this is also true for the surge-pitch and sway-roll coupled motions. Due to symmetry, damping in pure surge and sway motions is identical; similarly, damping in pure roll and pitch motions is identical. For the platform, wave-radiation damping in heave, roll and pitch motions is small compared to the damping in surge, sway, and yaw motions.

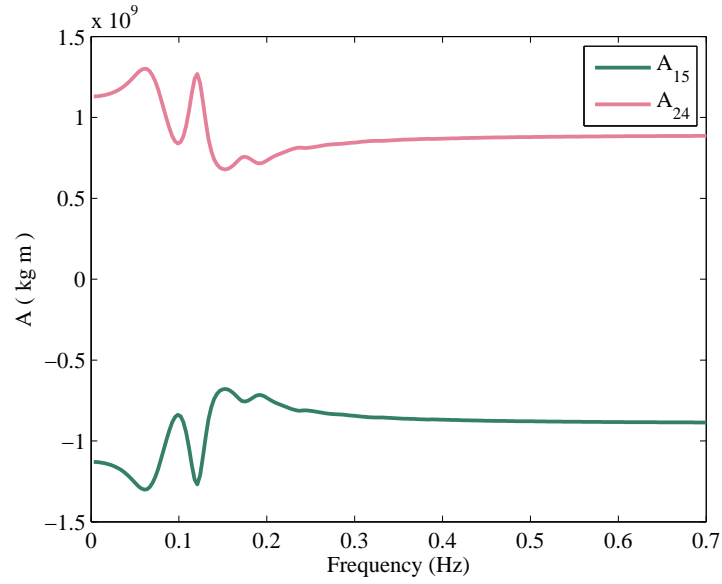


(a) Wave-damping coefficients for translational motions.

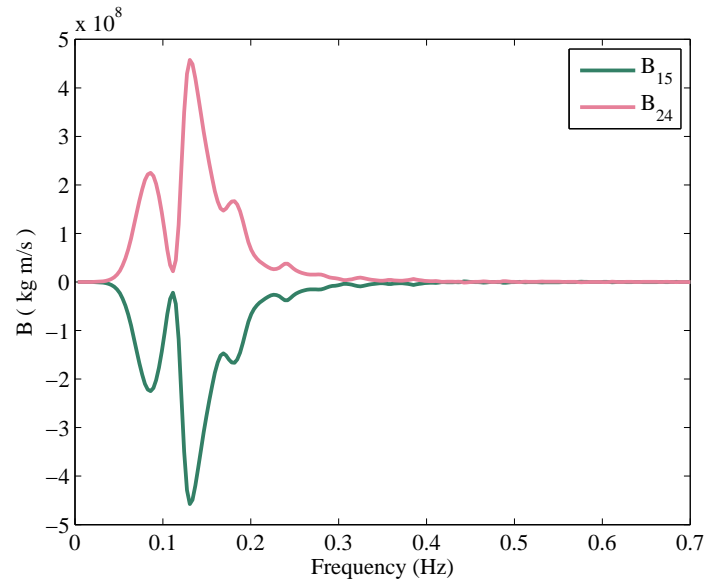


(b) Wave-damping coefficients for rotational motions.

Figure 3.7: Wave-radiation damping coefficients for the six degrees of freedom of the semi-submersible platform.



(a) Added mass coefficients for coupled motions.



(b) Radiation damping coefficients for coupled motions.

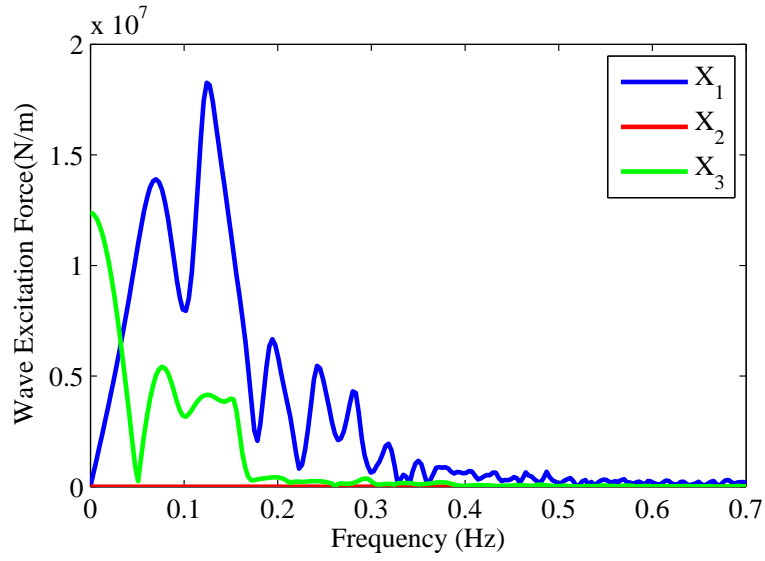
Figure 3.8: Hydrodynamic added mass and radiation damping coefficients for coupled modes of the semi-submersible platform.

### **3.5.3 Hydrodynamic wave excitation forces**

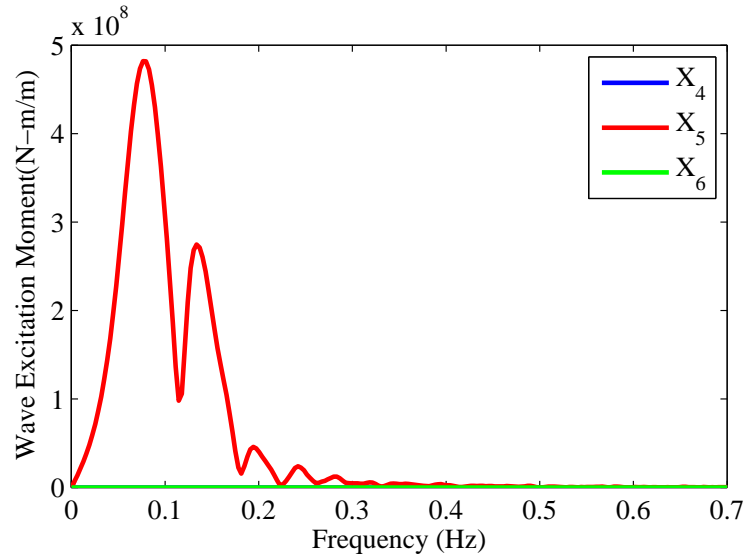
Hydrodynamic wave excitation forces for the six degrees of freedom are shown as functions of wave frequency in Figure 3.9. Since the wave propagates towards the platform with at a zero-degree wave heading, surge, heave, and pitch motions are most significant. Surge and pitch motions are coupled while heave forces result from the wave elevation. Wave forces in sway, roll, and yaw are zero because the incident wave is only along the positive  $x$  direction. Heave forces are greatest at very low frequencies. Except at very low frequencies, compared to other degrees of freedom, wave excitation forces in surge are highest even at relatively high wave frequencies.

## **3.6 WAMIT and MultiSurf Files**

In Appendix A, relevant MultiSurf and WAMIT files are listed. The MultiSurf files needed for the WAMIT analyses and other WAMIT input and output files are included. WAMIT output files are needed for FAST.



(a) Wave excitation forces in the direction of translational motions.



(b) Wave excitation moments in the direction of rotational motions.

Figure 3.9: Wave excitation forces for the six degrees of freedom of the semi-submersible platform.

## **Chapter 4**

### **Response Analyses for the OC4 5 MW and the 13.2 MW Wind Turbines**

In the wind energy industry, through several years of research and development, various types of floating offshore wind turbines have been studied and developed. They include spar buoys, tension leg platforms, barges, and semi-submersible platforms. The OC4 semi-submersible floating platform was developed to supporting the NREL 5 MW. The platform model used in this study is scaled up and adapted from OC4 in order to support the Sandia 13.2 MW wind turbine.

Semi-submersible platforms can be comprised of multiple members; for the 13.2 MW turbine, the platform includes a main column, three offset columns, cross-frame members, and pontoons as was described in Section 2.4. The presence of multiple separated members as part of the semi-submersible platform offers large restoring inertias due to large water plane area and the large moment arms associated with the offset columns. This leads to different behavior than is seen with spar buoys or TLPs that usually have only a single central supporting structural member. Nonlinear hydrodynamic loads due to waves are important for semi-submersible platforms. FAST version

8 [15] has the capability to model multiple members in response calculations.

In this chapter, the steady-state platform response to regular waves is studied for the OC4 semi-submersible platform and the semi-submersible platform model developed for the 13.2 MW wind turbine. These studies help to understand the behavior of the large-scale 13.2 MW wind turbine system in comparison with the widely studied 5 MW turbine and OC4 semi-submersible platform. These steady-state time-domain analyses can be helpful in understanding the behavior of the integrated turbine-platform-mooring system when exposed to turbulent wind fields and irregular waves.

## **4.1 Important Modeling Considerations**

For modeling a floating semi-submersible platform, potential flow theory and strip theory are essential [1]. WAMIT uses potential flow theory to produce linear hydrodynamic analysis results in the form of added-mass, wave-radiation damping, wave excitation, and hydrostatic restoring coefficients; computation is for regular waves only. Hydrodynamic analysis results from WAMIT simulations were discussed in Section 3.5. Nonlinear hydrodynamic effects based on strip theory are accounted for in FAST.

### **4.1.1 Linear hydrodynamics with potential flow**

Hydrodynamic coefficients for the floating platform model generated by WAMIT, using potential flow theory to solve the linear hydrodynamics



problem, were discussed in Chapter 3. FAST couples the floating platform with the turbine and mooring systems using the HydroDyn module, for which added-mass coefficients, wave radiation damping coefficients, wave excitation forces, and hydrostatic restoring stiffnesses are all needed as inputs.

#### **4.1.2 Nonlinear Hydrodynamics**

Morison’s equation is used to calculate hydrodynamic loads on the platform when flow separation occurs around the members of the platform. In such cases, the linear hydrodynamic loads from potential flow theory are negligible. Morison’s equation accounts for wave loading from the incident wave-induced excitation, radiation-induced inertial added mass, and flow separation-induced viscous drag forces [1].

Hydrodynamic inertial and viscous drag coefficients for each member can be defined in the HydroDyn module for FAST version 8. The semi-submersible platform will have different inertial and drag coefficients for members experiencing different exposure to waves. Upper columns encounter waves in a transverse direction, like a cylinder in cross-flow waves; drag coefficients can be determined based on the relevant Reynolds number [1]. Forces on the base columns, which act as heave plates, cannot be calculated based on the Reynolds number; inertial and drag coefficients can be estimated using wave tank test data. It has been suggested that for both the upper and the base columns, inertial and drag coefficients should be based on wave tank test data [1]. In this study, we assume added mass (inertial) and

drag coefficients for the 13.2 MW semi-submersible platform are the same as those for the OC4 platform.

## **4.2 Steady-State Response of the Semi-Submersible Platform under Regular Waves**

We are interested in understanding the behavior of the semi-submersible platform under different loading conditions. Studying the steady-state response of the platform under regular waves helps to understand the platform behavior; this is possible using linear hydrodynamic analysis results derived from WAMIT. For analysis using regular waves, the system is excited by a sinusoidal wave of 1-meter amplitude (2-meter wave height) and different wave periods. The relative influence of waves of different wave periods or frequencies can be understood in terms of Response Amplitude Operator (RAOs). Frequency-dependent RAOs describe the amplitude of the response (e.g., a displacement or rotation) under a wave of unit amplitude. To evaluate the full-system RAOs for the platform's six degrees of freedom, simulations are performed and platform motion amplitudes studied in the time domain using FAST for unit-amplitude waves [13]. The steady-state response amplitude is the converged response after transients have died out. RAOs for the OC4 platform model and for the 13.2 MW semi-submersible platform model are discussed next.

#### 4.2.1 Steady-State Platform Motion Time Series

Sinusoidal waves with unit amplitude are applied in order to study the OC4 semi-submersible platform's steady-state response. These analyses are performed in FAST and include 1,600 seconds of simulation without any winds and current. Initial conditions for the system are assigned as follows: the initial rotor speed is set at 9 rpm and the initial platform surge and pitch are set at 5 m and 1.9 degrees, respectively. Time series of the OC4 platform response at a wave frequency of 0.0092 Hz are shown in Figure 4.1. The WaveElev time series shows the unit-amplitude sea surface (wave) elevation process with a period of 108 seconds. The surge and heave response follow the wave time series with the same period and phase, whereas the pitch and yaw response processes have the same period but slightly different phases relative to the wave. The sway and roll response appear to decay to very low steady-state levels. The amplitude of the heave response is about 1 meter for waves with a period of 108 seconds; this is similar to the response of a particle moving vertically due to regular waves. The platform response levels are sometimes large while transients are present but they decay due to damping until a steady-state periodic level is reached. Each platform degree of freedom shows slightly different decay rates due to damping—for instance, surge motions show little effects of damping because the incident wave frequency is very close to the surge natural frequency. Platform sway, roll, and yaw show relatively larger effects of damping that ultimately suppress transient effects.

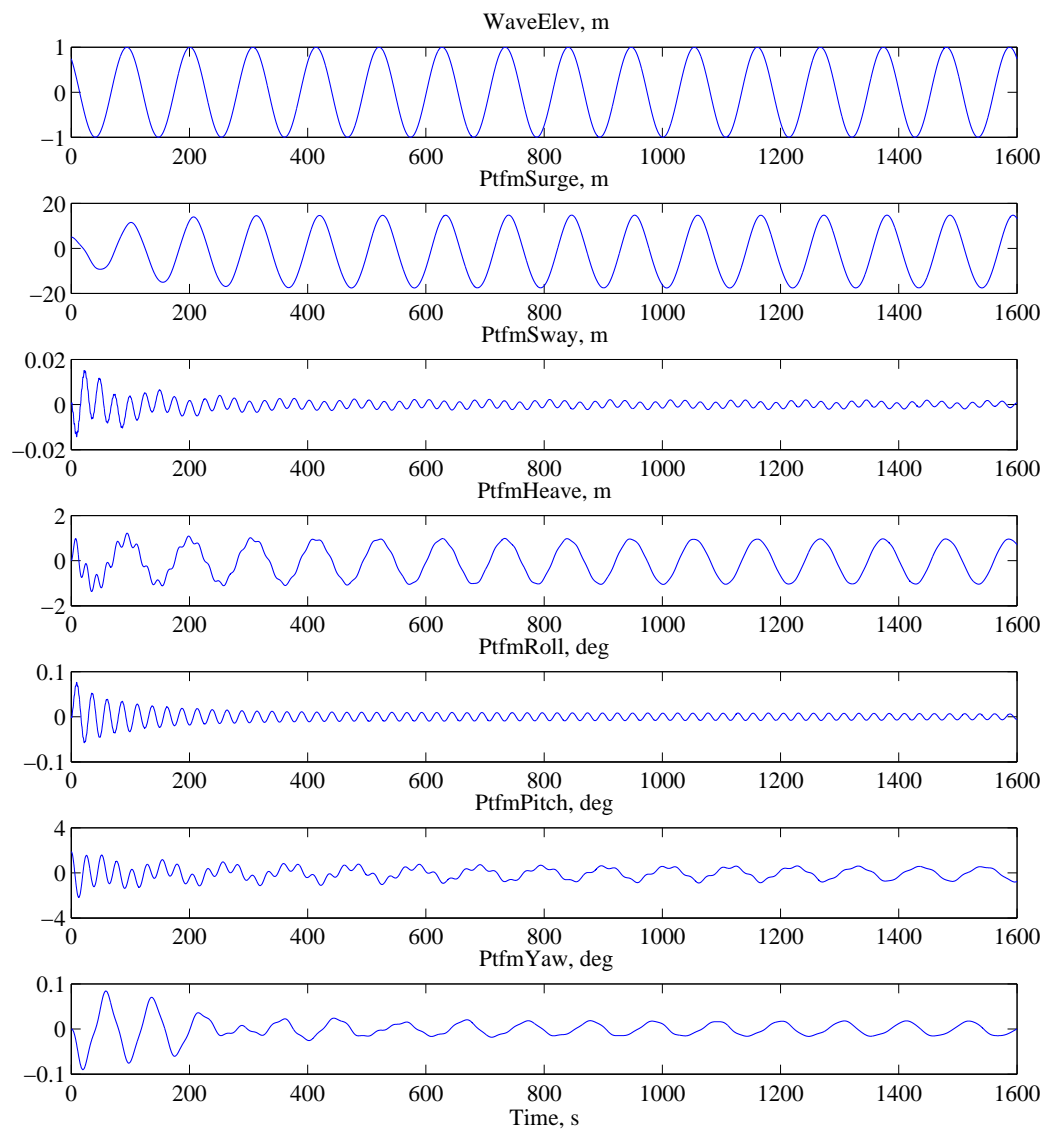


Figure 4.1: Time series of the OC4 platform steady-state response for a unit-amplitude wave at the surge natural frequency.

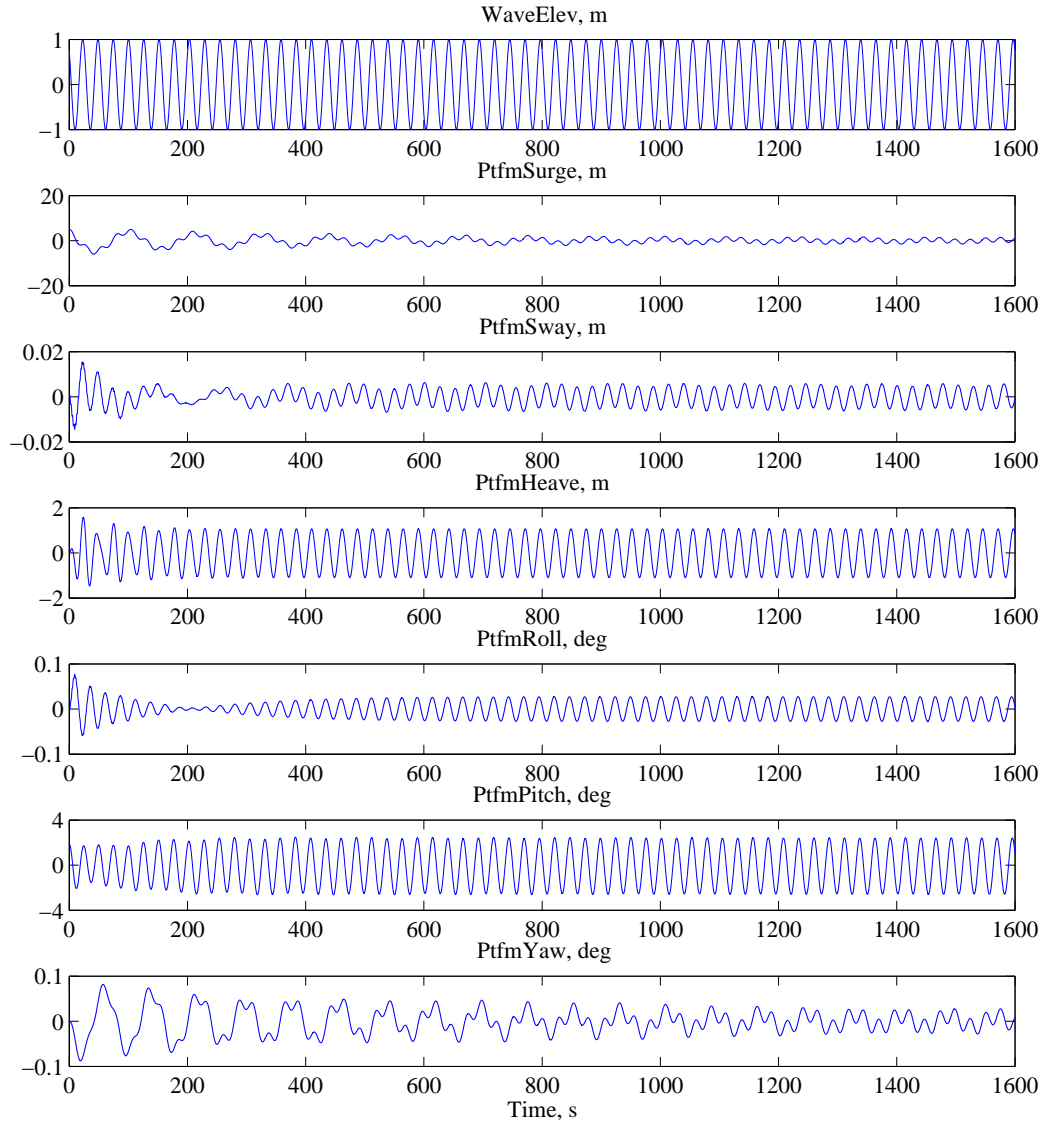


Figure 4.2: Time series of the OC4 platform steady-state response for a unit-amplitude wave at the pitch natural frequency.

Time series of the OC4 platform response at a wave frequency of 0.0395 Hz (close to the platform's pitch natural frequency) are shown in Figure 4.2. These can directly compared with the platform response for waves close to the surge natural wave frequency that were presented in Figure 4.1. The wave period now is approximately 25 seconds; the platform's pitch and heave behavior show similar characteristics; these motions have almost the same period and phase as the input wave. The sway and roll motions are larger compared to what was observed for waves close to the surge natural frequency. Heave motions again have unit amplitude but the response cycles are at the higher wave frequency. Since the wave frequency is equal to the pitch natural frequency, pitch motions are amplified due to resonance. Surge motions are considerably smaller than were observed for waves at the surge natural frequency. The platform yaw response shows energy at the pitch natural frequency due to coupling of these motions.

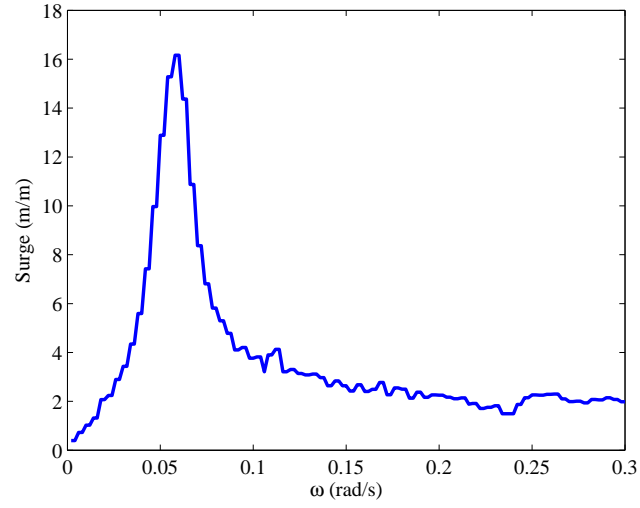
The amplitude of the different platform steady-state is calculated from the time series after the transients have died out. Since the input wave had a unit amplitude, the response amplitude directly yields the RAO at the specified wave frequency. To construct RAOs for the platform degrees of freedom as a function of frequency, FAST was run for regular waves with frequencies from 0.002 rad/s to 0.3 rad/s in increments of 0.002 rad/s. At each frequency, the steady-state periodic response for the six platform degrees of freedom was used to compute RAOs.

#### **4.2.2 RAOs for Motions of the OC4 5 MW Turbine and the 13.2 MW Turbine Semi-Submersible Platforms**

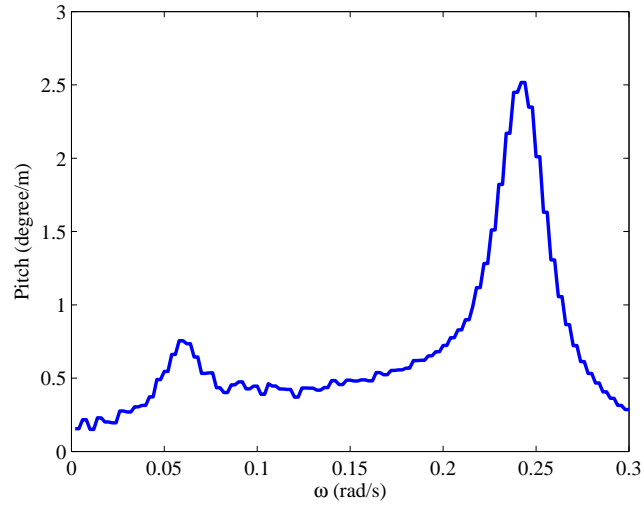
RAOs for platform surge and pitch motions for the OC4-5 MW turbine and the 13.2 MW turbine are shown in Figures 4.3 and 4.4. These RAOs are focused on low wave frequencies; platform motions of the OC4-5 MW turbine model are significantly larger than those for the 13.2 MW turbine model because the OC4 platform is significantly smaller. The 13.2 MW turbine's platform model has relatively much larger hydrostatic restoring coefficients and hydrodynamic coefficients that are also quite different from those for the OC4 platform model. In Figure 4.3(b), the coupling of surge and pitch motions is evident at frequency of around 0.058 rad/s for the OC4 platform. For the 13.2 MW turbine's platform model, the surge natural frequency is relatively much lower and its coupling effect on pitch is not as evident. A slight coupling effect of platform pitch on surge can be seen at a wave frequency of around 0.2 rad/s for the 13.2 MW turbine's platform. Surge and pitch natural frequencies for models of the OC4-5 MW turbine's platform and the 13.2 MW turbine's platform are listed in Table 4.1.

In summary, RAOs 13.2 MW turbine's semi-submersible platform are significantly smaller than those for the OC4-5 MW wind turbine's platform because the size of the larger turbine's platform considerably larger for the same incident waves. Once wind and current loads are applied and wave heights increased, platform responses for the 13.2 MW wind turbine are

expected to be greater under the combined effects of winds, waves, and currents.



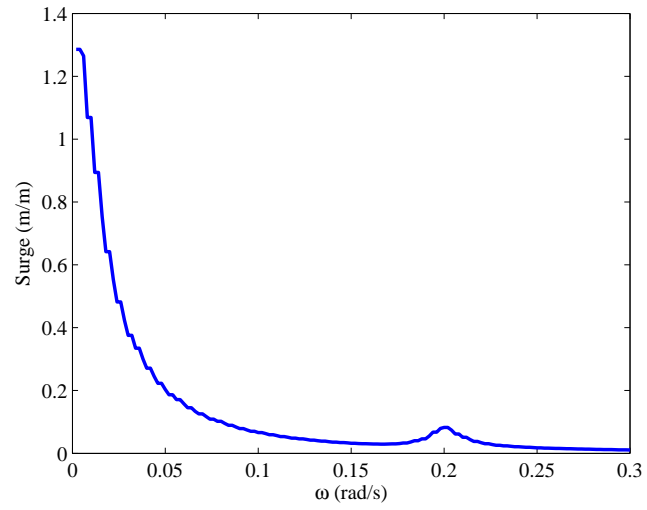
(a) RAO of surge



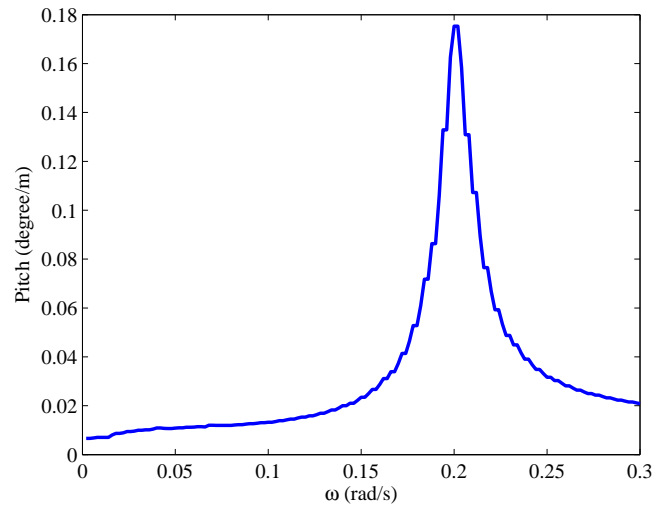
(b) RAO of pitch

Figure 4.3: RAOs for surge and pitch motions for the OC4 semi-submersible platform.





(a) RAO of surge



(b) RAO of pitch

Figure 4.4: RAOs for surge and pitch motions for the 13.2 MW turbine semi-submersible platform.

Table 4.1: Surge and pitch natural frequencies for the semi-submersible platform models.

Degree of Freedom	Natural Frequency (rad/s, Hz)	
	OC4-5 MW turbine	13.2 MW turbine
Surge	0.058, 0.0092	0.002, 0.00032
Pitch	0.248, 0.0395	0.2, 0.0318

### 4.3 Response of 13.2 MW Turbine to Irregular Waves and Turbulent Wind Fields

To understand the behavior of the 13.2 MW turbine-platform-mooring system under operating conditions, the response of the integrated system is studied for turbulent wind fields and irregular waves for a reference site with 200-m water depth. Figures 4.5 and 4.6 show response time series for a 10-minute segment and for a full 1-hour simulation of the most severe sea state at the selected reference site [23] for which available metocean data on wind and waves were obtained. The site is situated close to Half Moon Bay, near San Francisco, California and has a water depth very close to 200 meters. The sea state chosen has a average wind speed of 23 m/s at hub height ( $V_{hub} = 23$  m/s), a significant wave height of 5.5 meters ( $H_s = 5.5$  m), and a peak spectral wave period of 11 seconds ( $T_p = 11$  sec). Response simulations were performed using FAST; the wind field was generated using TurbSim assuming IEC turbulence category ‘B’ applies [20]. The non-zero mean wind field is in the longitudinal direction (along the positive  $x$ -axis). Irregular wave are generated using a

JONSWAP spectrum with  $H_s = 5.5$  m and  $T_p = 11$  s [36] and are also directed along the positive  $x$ -axis (i.e., aligned with the mean wind field).

From Figure 4.5, it can be seen that large blade pitch angles result due to the high hub-height mean wind speed of 23 m/s, which is well above the turbine rated wind speed of 11.3 m/s. The tower base fore-aft bending moment (TwrBsMyt) appears to follow the wind and is also coupled with the platform's pitch motion. The platform pitch response is mainly driven by wave loading. The platform surge appears to follow the large aerodynamic loading on the wind turbine which pushes the system to a surge offset, while feeling the influence of blade pitching which controls the aerodynamic loads on the turbine. Forces at an anchor point of the mooring system are zero suggesting no uplift at the anchor, which is a design concern for a catenary mooring system. In Figure 4.6, a full 1-hour simulation is shown that describes the response of the integrated system. It can be seen that the platform surge, which is closely related to the wind loading, is significantly influenced by the blade pitch angle. The longer time series are helpful in understanding the system response for offshore wind turbines that have low natural frequencies such as for the platform surge motions.

Overall, the behavior of the integrated system suggests that the 13.2 MW offshore wind turbine, supported on the semi-submersible platform model developed in this study, experiences loads that are within acceptable limits. The selected site with a water depth of 200 m, however, experiences very small wave heights. This is one of the reasons why the system response

levels are low. At other potential sites even for the same water depth, the integrated wind turbine-platform-mooring system might experience more severe environmental conditions. The 13.2 MW offshore wind turbine has the capability to produce more power than other existing wind turbines; hence, additional investigation into the behavior of this offshore wind turbine (with the same supporting platform and mooring system) at different sites with possibly higher wind and wave loading is recommended.

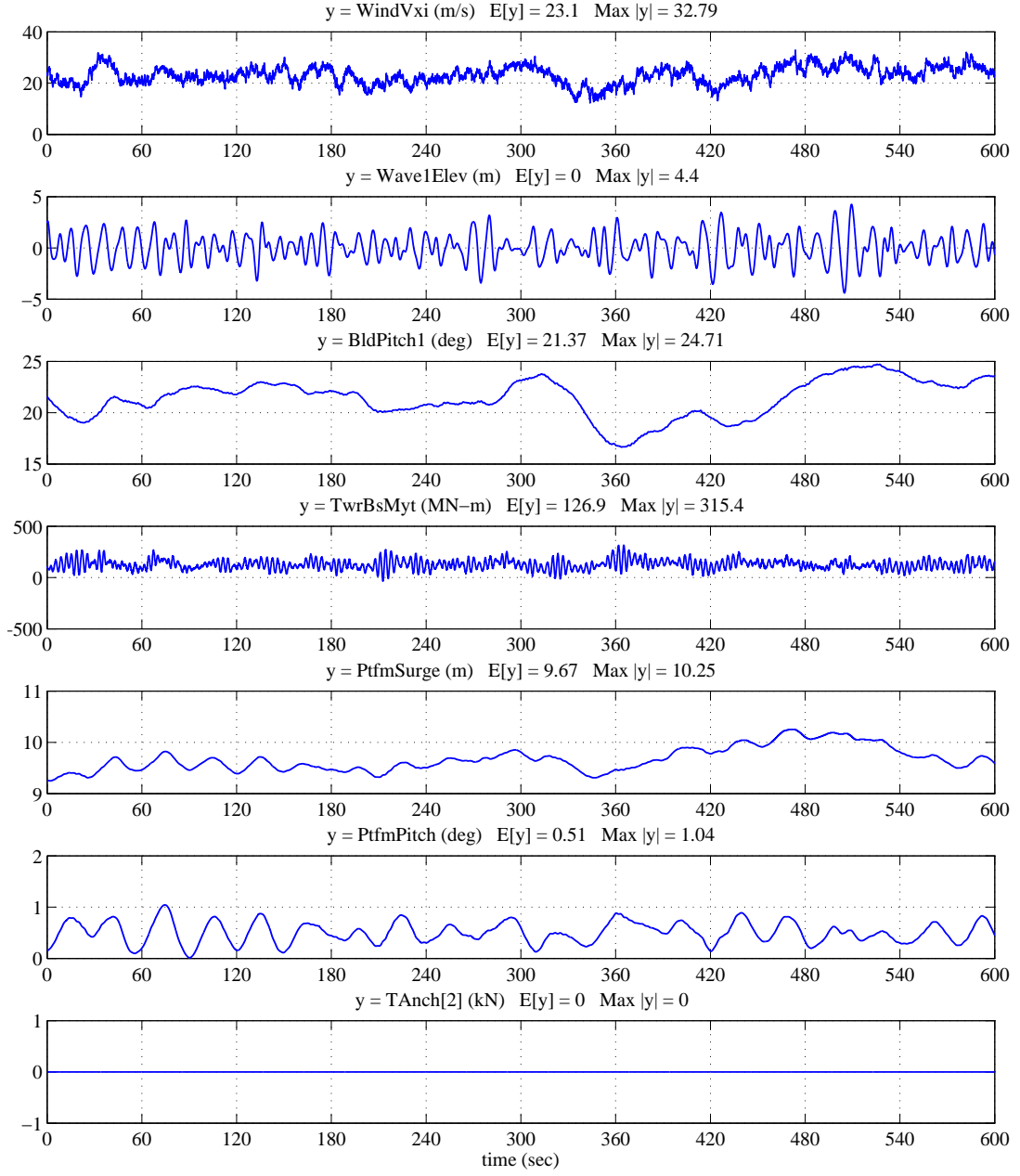


Figure 4.5: Time series highlighting 10-minute segments of the simulated response of the 13.2 MW wind turbine-platform-mooring system given  $V_{hub} = 23$  m/s,  $H_s = 5.5$  m, and  $T_p = 11$  s.

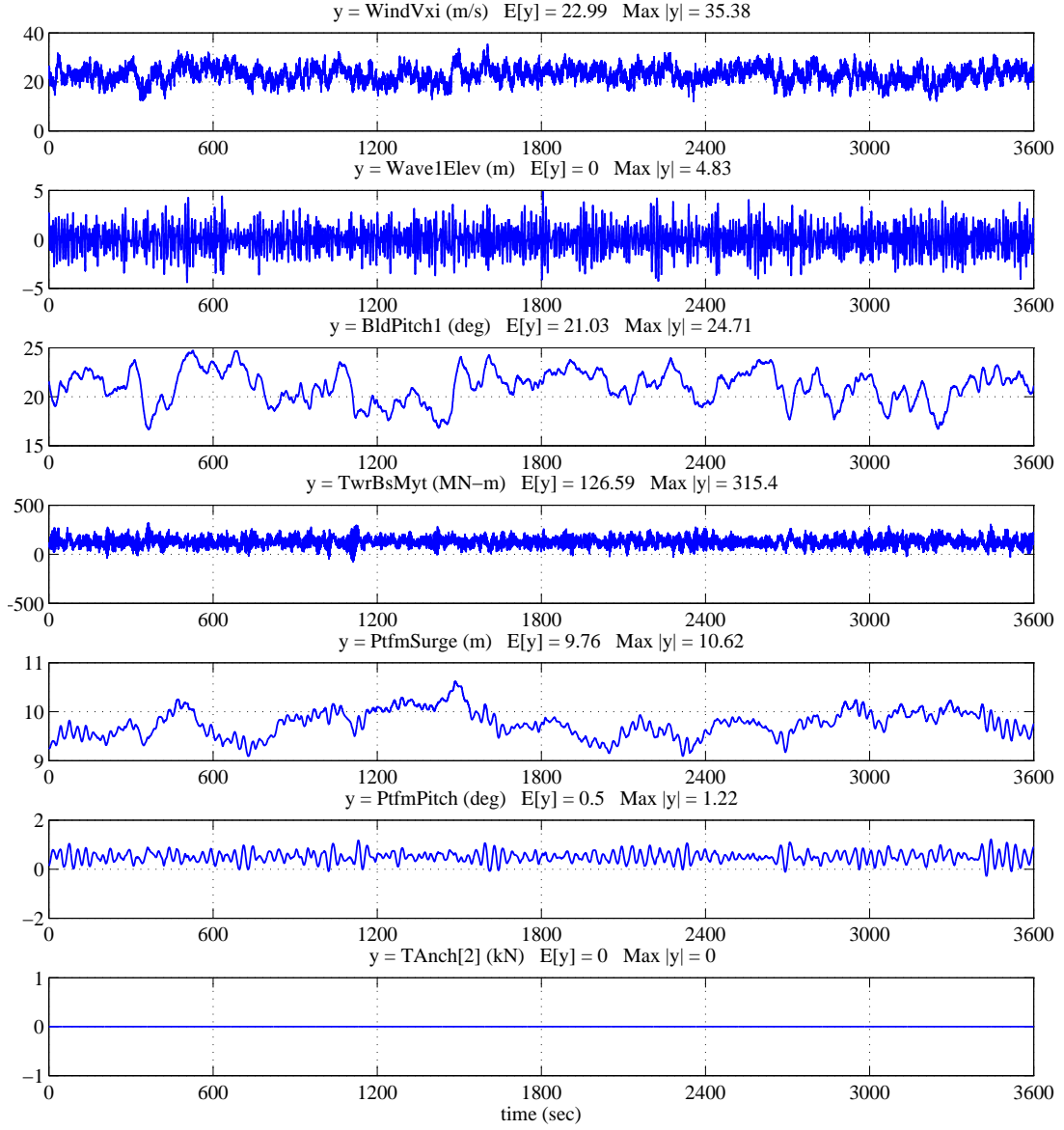


Figure 4.6: One-hour time series of the simulated response of the 13.2 MW wind turbine-platform-mooring system given  $V_{hub} = 23$  m/s,  $H_s = 5.5$  m, and  $T_p = 11$  s.

## **4.4 TurbSim and FAST Files**

In Appendix A, relevant input files used in example TurbSim and FAST simulations are listed. TurbSim output files are needed in the FAST simulations. WAMIT output files are also needed for the HydroDyn module computations in FAST.

## **4.5 Summary**

For both regular waves and for irregular waves with turbulent wind fields, response levels of the integrated 13.2 MW turbine-platform-mooring system was found to rather low. The platform model is probably over-designed as scaling was based on considerations of the maximum fore-aft bending moment at the base of tower. While not the focus of the present study, in future work, the platform dimensions could be optimized to produce a more efficient and economical design.

## Chapter 5

### Conclusions

#### 5.1 Overview of the Research Study

Over the last few decades, offshore wind turbines have been extensively studied and are being thought of as a viable renewable energy source. Research studies suggest that deepwater sites may offer some advantages especially in the size of turbines that can be deployed there. Floating offshore wind turbines are the preferred choice for such deepwater sites. Depending on the type of supporting platform and site conditions, several considerations are important; this is the case, for example, in designing an integrated turbine, mooring system, and floating semi-submersible platform. Researchers at Sandia National Laboratories have developed a large 13.2 MW wind turbine model with 100-meter blades. This research study discussed the development of a buoyancy-stabilized semi-submersible platform and mooring system to support this large wind turbine. Hydrodynamic loads on the platform were studied under both regular and irregular wave excitation. Linear and nonlinear hydrodynamic effects on the platform were accounted for in the model development.



## 5.2 Conclusions

A semi-submersible platform model was developed to support the 13.2 MW wind turbine; a catenary mooring system was also designed. The platform was modeled and only linear hydrodynamics based on potential flow theory was considered. Nonlinear hydrodynamics based on strip theory was also considered. To understand the behavior of the integrated system, comparisons were made with the response of the OC4 Phase II design with a 5 MW turbine and a semi-submersible platform. From the various analysis conducted, the following conclusions are drawn:

- In the semi-submersible platform design, motions resulting from consideration of the added mass, wave-radiation damping, and wave excitation from hydrodynamic radiation and diffraction became significant when the platform was excited by low-frequency waves.
- It was necessary to modify the offshore turbine's pitch control and variable speed control parameters. This was done to prevent negative damping on the platform.
- The platform was modeled using MultiSurf. A high-order surface was created using B-Splines for use with WAMIT. This resulted in more accurate results than would be possible with lower-order surface definitions. An appropriate mesh size is required for reduced processing time in WAMIT and to ensure accuracy of the results.

- Added mass and damping coefficients of the platform for pure surge and pure sway motions were found to be identical; similarly pure roll and pure pitch motions had identical coefficients. This is due to the symmetry planes of the platform. Added mass coefficients in the heave direction were greater than those in surge and sway. This is due to the increase area of the wetted surface in the heave direction. At low and high wave frequencies, damping coefficients were almost zero for all six platform degrees of freedom.
- Significant wave-induced motions were in surge, heave, and pitch. Wave forces in surge were larger over a broader range of wave frequencies and especially so for waves with high frequencies. This is due to the short wavelengths of such high-frequency waves that cause greater diffraction effects.
- Hydrodynamics of the semi-submersible platform required inclusion of linear hydrodynamics as well as nonlinear hydrodynamics (inertial and viscous drag forces) for multiple members.
- The steady-state response of the floating platform was simulated for unit-amplitude regular waves at various frequencies. The responses showed some variation until the transients damped out and the steady-state periodic response was reached. Platform surge motion for waves close to the surge natural frequency showed some amplification as would be expected.

- The steady-state response of the OC4-5 MW wind turbine platform and the 13.2 MW turbine platform model were compared. Response Amplitude Operators (RAOs) for the larger turbine platform model were significantly lower than those for the OC4 platform model. This was largely because of the greater size of the 13.2 MW's supporting platform for similar waves.
- The integrated system response for an operating 13.2 MW turbine with platform and mooring system was simulated using FAST for turbulent wind fields and irregular waves. Wind speed and wave heights for a selected sea state were based on data from a reference site in the San Francisco area [23]. Overall, the system response levels were very low. The platform design can probably be refined to reduce geometrical dimensions, materials, and costs. Further study on the appropriate mooring system is also recommended.

### 5.3 Suggestions for Future Research

The present study represents an initial attempt at the development of a semi-submersible platform to support a large (13.2 MW) turbine. There are several limitations in the model development, mainly due to the lack of available data. Access to wave-tank test data would be very useful in validating the WAMIT hydrodynamic analysis results generated for this model. The preliminary model developed here was based on many assumptions; the assumptions included assuming a scaled-up size of the

platform from the OC4 model based on tower base moment considerations, non-optimized turbine controller parameters, and omission of second-order hydrodynamic coefficients. A study of different sizes of platform models to support the 13.2 MW wind turbine is recommended. The effects of inertia and viscous drag force from multiple members can be validated using the wave-tank test data, if these were available. The dynamics of the mooring system should be studied and compared with quasi-static assumptions; shorter and more high-tensioned mooring systems might suppress platform motions.

Once a refined model is developed, detailed studies of extreme and fatigue loads can be undertaken and various limit states examined. Long-term loads can be assessed by systematic study of all sea states of interest.

## Appendix

# Appendix A

## Model Files

### A.1 MultiSurf Output Files for WAMIT

```
Input file: SNL_semi_finer.gdf
Model SNL_SEMI_FINER
1.000000 9.806650 ULEN, GRAV
0 1 ISX, ISY
0 2 NPATCH IGDEF
3 NLINES
SNL_SEMI_FINER.MS2
*
0 0 0 Fast/acc DivMult Inward_normals
```

```
Input file: SNL_semi_finer.pot
SNL_semi_finer.pot, ILOWHI=1, IRR=1
200 HBOT
1 1 IRAD, IDIFF
-250 NPER
0.02 0.02 PER
1 NBETA
0 BETA
1 NBODY
SNL_semi_finer.gdf
0. 0. 0. 0.0 XBODY(1-4)
1 1 1 1 1 1 IMODE(1-6)
```

```
Input file: SNL_semi_finer.cfg
ipltdat=5
ISOR=0
ISOLVE=1
ISCATT=0
ILOG=1
IRR=1
IPERIN=2
IPEROUT=2
ILOWHI=1
ILOWGDF=1
PANEL_SIZE=2.0
NUMHDR=1
USERID_PATH=\wamitv7
```

```
Input file: SNL_semi_finer.frc
```

```

SNL_semi_finer.frc, ILOWHI=1, IRR=1
1 0 1 0 0 0 0 0 0 IOPTN(1-9) (Required Output Files)
0.0 VCG
0.000000 0.000000 0.000000
0.000000 0.000000 0.000000
0.000000 0.000000 0.000000 XPRDCT
0 NBETAH
0 NFIELD

```

## A.2 Additional WAMIT Input Files

```

Input file: config.wam
! generic configuration file: config.wam
RAMGBMAX=16
NCPU=5
USERID_PATH=\wamitv7
LICENSE_PATH=\wamitv7\license

```

```

Input file: fnames.wam
SNL_semi_finer.cfg
SNL_semi_finer.gdf
SNL_semi_finer.pot
SNL_semi_finer.frc

```

## A.3 Sample of WAMIT Output Files for HydroDyn Inputs

```

Output file: SNL_semi_finer.hst
1 1 0.000000E+00
1 2 0.000000E+00
1 3 0.000000E+00
1 4 0.000000E+00
1 5 0.000000E+00
1 6 0.000000E+00
2 1 0.000000E+00
2 2 0.000000E+00
2 3 0.000000E+00
2 4 0.000000E+00
2 5 0.000000E+00
2 6 0.000000E+00
3 1 0.000000E+00
3 2 0.000000E+00
3 3 1.231475E+03
3 4 0.000000E+00
3 5 2.358674E-01
3 6 0.000000E+00
4 1 0.000000E+00
4 2 0.000000E+00
4 3 0.000000E+00
4 4 -3.976515E+05
4 5 0.000000E+00
4 6 0.000000E+00

```

5	1	0.000000E+00
5	2	0.000000E+00
5	3	2.358674E-01
5	4	0.000000E+00
5	5	-3.976644E+05
5	6	0.000000E+00
6	1	0.000000E+00
6	2	0.000000E+00
6	3	0.000000E+00
6	4	0.000000E+00
6	5	0.000000E+00
6	6	0.000000E+00

Output file: SNL\_semi\_finer.1

-0.100000E+01	1	1	4.976386E+04	
-0.100000E+01	1	3	-1.142347E-01	
-0.100000E+01	1	5	-1.101204E+06	
-0.100000E+01	2	2	4.975876E+04	
-0.100000E+01	2	4	1.101273E+06	
-0.100000E+01	2	6	1.315589E+02	
-0.100000E+01	3	1	1.485088E-01	
-0.100000E+01	3	3	8.494051E+04	
-0.100000E+01	3	5	2.200705E+02	
-0.100000E+01	4	2	1.101318E+06	
-0.100000E+01	4	4	1.404572E+08	
-0.100000E+01	4	6	7.074045E+03	
-0.100000E+01	5	1	-1.101544E+06	
-0.100000E+01	5	3	4.300016E+02	
-0.100000E+01	5	5	1.404221E+08	
-0.100000E+01	6	2	1.056935E+02	
-0.100000E+01	6	4	-1.848778E+03	
-0.100000E+01	6	6	1.184900E+08	
0.000000E+00	1	1	3.690174E+04	
0.000000E+00	1	3	-7.193954E-02	
0.000000E+00	1	5	-8.709586E+05	
0.000000E+00	2	2	3.690329E+04	
0.000000E+00	2	4	8.709556E+05	
0.000000E+00	2	6	-3.305270E+01	
0.000000E+00	3	1	4.110625E-01	
0.000000E+00	3	3	8.373952E+04	
0.000000E+00	3	5	1.342304E+02	
0.000000E+00	4	2	8.709589E+05	
0.000000E+00	4	4	1.328110E+08	
0.000000E+00	4	6	-1.499344E+03	
0.000000E+00	5	1	-8.709691E+05	
0.000000E+00	5	3	2.235323E+02	
0.000000E+00	5	5	1.327670E+08	
0.000000E+00	6	2	-3.341485E+01	
0.000000E+00	6	4	6.631035E+02	
0.000000E+00	6	6	8.971874E+07	
0.100000E-02	1	1	4.979093E+04	5.523158E-03
0.100000E-02	1	3	1.818223E-01	-2.266286E-01
0.100000E-02	1	5	-1.101849E+06	-5.415985E-02
0.100000E-02	2	2	4.978593E+04	5.529084E-03
0.100000E-02	2	4	1.101912E+06	6.298102E-02
0.100000E-02	2	6	1.358103E+02	6.682801E-04



0.100000E-02	3	1	1.251085E+00	2.658467E-02
0.100000E-02	3	3	9.151975E+04	1.892287E+03
0.100000E-02	3	5	2.722076E+02	-9.818535E-01
0.100000E-02	4	2	1.101664E+06	5.628557E-02
0.100000E-02	4	4	1.404619E+08	9.752976E-01
0.100000E-02	4	6	7.062504E+03	-5.333903E-01
0.100000E-02	5	1	-1.101875E+06	7.298774E-02
0.100000E-02	5	3	4.472153E+02	-1.245567E+00
0.100000E-02	5	5	1.404240E+08	-5.883082E-01
0.100000E-02	6	2	9.745033E+01	-5.021530E-04
0.100000E-02	6	4	-2.070452E+03	-3.192261E-02
0.100000E-02	6	6	1.184898E+08	1.282031E-01
0.200000E-02	1	1	4.979114E+04	2.319381E-02
0.200000E-02	1	3	-4.010419E-01	-2.741593E-01
0.200000E-02	1	5	-1.101848E+06	-1.710671E-01
0.200000E-02	2	2	4.978597E+04	2.171036E-02
0.200000E-02	2	4	1.101914E+06	2.527806E-01
0.200000E-02	2	6	1.356572E+02	8.653136E-05
0.200000E-02	3	1	1.871337E-01	-2.411114E-02
0.200000E-02	3	3	9.068594E+04	1.892142E+03
0.200000E-02	3	5	2.249504E+02	4.592268E-01
0.200000E-02	4	2	1.101670E+06	2.459354E-01
0.200000E-02	4	4	1.404622E+08	7.497533E-02
0.200000E-02	4	6	7.039974E+03	-1.383172E-01
0.200000E-02	5	1	-1.101850E+06	-2.444340E-01
0.200000E-02	5	3	2.630797E+02	2.514381E-01
0.200000E-02	5	5	1.404251E+08	4.220884E+00
0.200000E-02	6	2	9.811125E+01	1.921520E-04
0.200000E-02	6	4	-2.098705E+03	-8.012299E-03
0.200000E-02	6	6	1.184901E+08	-4.526034E-01
.				
.				
0.500000E+01	6	6	8.846572E+07	1.115900E+05

Output file: SNL\_semi\_finer.3

0.100000E-02	0.000000E+00	1	2.957571E+00	8.892072E+01	5.570840E-02	2.957046E+00
0.100000E-02	0.000000E+00	2	0.000000E+00	9.000000E+01	0.000000E+00	0.000000E+00
0.100000E-02	0.000000E+00	3	1.231196E+03	1.078936E-05	1.231196E+03	2.318463E-04
0.100000E-02	0.000000E+00	4	0.000000E+00	9.000000E+01	0.000000E+00	0.000000E+00
0.100000E-02	0.000000E+00	5	3.450163E+01	-1.010286E+02	-6.600154E+00	-3.386444E+01
0.100000E-02	0.000000E+00	6	0.000000E+00	9.000000E+01	0.000000E+00	0.000000E+00
0.200000E-02	0.000000E+00	1	5.914502E+00	8.938275E+01	6.371562E-02	5.914158E+00
0.200000E-02	0.000000E+00	2	0.000000E+00	9.000000E+01	0.000000E+00	0.000000E+00
0.200000E-02	0.000000E+00	3	1.231145E+03	3.998358E-05	1.231145E+03	8.591484E-04
0.200000E-02	0.000000E+00	4	0.000000E+00	9.000000E+01	0.000000E+00	0.000000E+00
0.200000E-02	0.000000E+00	5	6.809190E+01	-9.589921E+01	-6.998403E+00	-6.773130E+01
0.200000E-02	0.000000E+00	6	0.000000E+00	9.000000E+01	0.000000E+00	0.000000E+00
.						
.						
0.500000E+01	0.000000E+00	6	0.000000E+00	9.000000E+01	0.000000E+00	0.000000E+00

## A.4 TurbSim Input File

TurbSim Input File. Valid for TurbSim v1.06.00, 21-Sep-2012

```

-----Runtime Options-----
1837852201      RandSeed1      - First random seed (-2147483648 to 2147483647)
1283785352      RandSeed2      - Second random seed (-2147483648 to 2147483647)
False           WrBHHTP       - Output hub-height turbulence parameters in binary form?
False           WrFHHTP       - Output hub-height turbulence parameters in formatted
False           WrADHH        - Output hub-height time-series data in AeroDyn form?
False           WrADFF        - Output full-field time-series data in TurbSim/AeroDyn
True            WrBLFF        - Output full-field time-series data in BLADED/AeroDyn
False           WrADTWR       - Output tower time-series data? (Generates RootName.twr)
False           WrFMTFF       - Output full-field time-series data in formatted
False           WrACT         - Output coherent turbulence time steps in AeroDyn form?
True            Clockwise     - Clockwise rotation looking downwind?
0              ScaleIEC       - Scale IEC turbulence models to exact target standard

-----Turbine/Model Specifications-----
29              NumGrid_Z     - Vertical grid-point matrix dimension
29              NumGrid_Y     - Horizontal grid-point matrix dimension
0.1000          TimeStep      - Time step [seconds]
4000.0          AnalysisTime  - Length of analysis time series [seconds] (program will
4000.0          UsableTime    - Usable length of output time series [seconds] (program
146             HubHt         - Hub height [m] (should be > 0.5*GridHeight)
280             GridHeight    - Grid height [m]
280             GridWidth     - Grid width [m] (should be >= 2*(RotorRadius+ShaftLeng
0               VFlowAng      - Vertical mean flow (uptilt) angle [degrees]
0               HFlowAng      - Horizontal mean flow (skew) angle [degrees]

-----Meteorological Boundary Conditions-----
"IECKAI"        TurbModel     - Turbulence model ("IECKAI"=Kaimal, "IECVKM"=von Karman
"1-ED3"         IECstandard   - Number of IEC 61400-x standard (x=1,2, or 3 with
"B"             IECturbc      - IEC turbulence characteristic ("A", "B", "C" or the
"NTM"           IEC_WindType  - IEC turbulence type ("NTM"=normal, "xETM"=extreme
default         ETMc          - IEC Extreme Turbulence Model "c" parameter [m/s]
IEC             WindProfileType - Wind profile type ("JET";"LOG"=logarithmic;"PL"=power
146             RefHt         - Height of the reference wind speed [m]
23.0            URef          - Mean (total) wind speed at the reference height [m/s]
default         ZJetMax       - Jet height [m] (used only for JET wind profile, valid
default         PLExp         - Power law exponent [-] (or "default")
default         ZO            - Surface roughness length [m] (or "default")

-----Non-IEC Meteorological Boundary Conditions-----
default         Latitude      - Site latitude [degrees] (or "default")
0.05            RICH_NO       - Gradient Richardson number
default         UStar         - Friction or shear velocity [m/s] (or "default")
default         ZI            - Mixing layer depth [m] (or "default")
default         PC_UW         - Hub mean u'w' Reynolds stress (or "default")
default         PC_UV         - Hub mean u'v' Reynolds stress (or "default")
default         PC_VW         - Hub mean v'w' Reynolds stress (or "default")
default         IncDec1       - u-component coherence parameters (e.g. "10.0 0.3e-3"
default         IncDec2       - v-component coherence parameters (e.g. "10.0 0.3e-3"
default         IncDec3       - w-component coherence parameters (e.g. "10.0 0.3e-3"
default         CohExp        - Coherence exponent (or "default")

-----Coherent Turbulence Scaling Parameters-----

```

"Test\EventData\"	CTEventPath	- Name of the path where event data files are located
"Random"	CTEventFile	- Type of event files ("LES", "DNS", or "RANDOM")
true	Randomize	- Randomize the disturbance scale and locations?
1.0	DistScl	- Disturbance scale (ratio of wave height to rotor disk)
0.5	CTLy	- Fractional location of tower centerline from right
0.5	CTLz	- Fractional location of hub height from the bottom of
30.0	CTStartTime	- Minimum start time for coherent structures in

=====

NOTE: Do not add or remove any lines in this file!

=====

## A.5 FAST Input Files

### A.5.1 FAST

```

----- FAST v8.08.* INPUT FILE -----
SNL13.2-00-Floating Turbine Design Model SNL 13.2MW Turbine with SNL100-02 Baseline Blades
----- SIMULATION CONTROL -----
False      Echo          - Echo input data to <RootName>.ech (flag)
"FATAL"     AbortLevel   - Error level when simulation should abort (string)
4000.0      TMax         - Total run time (s)
0.0100      DT          - Recommended module time step (s)
2           InterpOrder  - Interpolation order for input/output time history (-)
0           NumCrctn     - Number of correction iterations (-)
999999      DT_UJac      - Time between calls to get Jacobians (s)
1E+06       UJacSclFact  - Scaling factor used in Jacobians (-)
----- FEATURE SWITCHES AND FLAGS -----
1  CompElast  - Compute structural dynamics (switch) {1=ElastoDyn; 2=ElastoDyn +
1  CompAero   - Compute aerodynamic loads (switch) {0=None; 1=AeroDyn}
1  CompServo  - Compute control and electrical-drive dynamics (switch) {0=None;
1  CompHydro  - Compute hydrodynamic loads (switch) {0=None; 1=HydroDyn}
0  CompSub    - Compute sub-structural dynamics (switch) {0=None; 1=SubDyn}
1  CompMooring - Compute mooring system (switch) {0=None; 1=MAP; 2=FEAMooring}
0  CompIce    - Compute ice loads (switch) {0=None; 1=IceFloe; 2=IceDyn}
False CompUserPtfmLd - Compute additional platform loading (flag)
False CompUserTwrLd  - Compute additional tower loading (flag)
----- INPUT FILES -----
"SNL13pt2_Floating_ElastoDyn.dat" EDFile      - Name of file containing ElastoDyn input
"unused"                          BDBldFile(1) - Name of file containing BeamDyn input
"unused"                          BDBldFile(2) - Name of file containing BeamDyn input
"unused"                          BDBldFile(3) - Name of file containing BeamDyn input
"SNL13pt2_Floating_AeroDyn.dat"   AeroFile    - Name of file containing aerodynamic
"SNL13pt2_Floating_ServoDyn.dat"  ServoFile   - Name of file containing control and
"SNL13pt2_Floating_HydroDyn.dat"  HydroFile   - Name of file containing hydrodynamic
"unused"                          SubFile      - Name of file containing sub-structural
"SNL13pt2_Floating_MAP.dat"       MooringFile  - Name of file containing mooring system
"unused"                          IceFile       - Name of file containing ice input
----- OUTPUT -----
True      SumPrint      - Print summary data to "<RootName>.sum" (flag)
50        SttsTime      - Amount of time between screen status messages (s)
0.02      DT_Out        - Time step for tabular output (s)
0         TStart        - Time to begin tabular output (s)
3         OutFileFmt     - Format for tabular (time-marching) output file (switch)
True      TabDelim       - Use tab delimiters in text tabular output file? (flag)

```

"ES10.3E2"      OutFmt      - Format used for text tabular output, excluding the time

## A.5.2 AeroDyn

### SNL13.2-Floating

SI	SysUnits	- System of units used for input and output [must be SI for FAST]
BEDDOES	StallMod	- Dynamic stall included [BEDDOES or STEADY] (unquoted string)
USE_CM	UseCm	- Use aerodynamic pitching moment model? [USE_CM or NO_CM]
EQUIL	InfModel	- Inflow model [DYNIN or EQUIL] (unquoted string)
SWIRL	IndModel	- Induction-factor model [NONE or WAKE or SWIRL] (unquoted string)
0.005	AToler	- Induction-factor tolerance (convergence criteria) (-)
PRANDtl	TLModel	- Tip-loss model (EQUIL only) [PRANDtl, GTECH, or NONE]
PRANDtl	HLModel	- Hub-loss model (EQUIL only) [PRANDtl or NONE] (unquoted string)
"Wind\TurbSim13pt2MW.wnd"	WindFile	- Name of file containing wind data
146.4	HH	- Wind reference (hub) height [TowerHt+Twr2Shft+OverHang*SIN
0.0	TwrShad	- Tower-shadow velocity deficit (-)
9999.9	ShadHWid	- Tower-shadow half width (m)
9999.9	T_Shad_Refpt	- Tower-shadow reference point (m)
1.225	AirDens	- Air density (kg/m <sup>3</sup> )
1.464E-5	KinVisc	- Kinematic air viscosity [CURRENTLY IGNORED] (m <sup>2</sup> /sec)
DEFAULT	DTAero	- Time interval for aerodynamic calculations (sec)
8	NumFoil	- Number of airfoil files (-)
"AeroData\Cylinder1.dat"		FoilNm
"AeroData\Cylinder2.dat"		
"AeroData\DU40_A17.dat"		
"AeroData\DU35_A17.dat"		
"AeroData\DU30_A17.dat"		
"AeroData\DU25_A17.dat"		
"AeroData\DU21_A17.dat"		
"AeroData\NACA64_A17.dat"		
18	BldNodes	- Number of blade nodes used for analysis (-)
RNodes	AeroTwst	DRNodes      Chord      NFoil      PrnElm
4.7222	13.308	4.4444      5.767      1      NOPRINT
9.1667	13.308	4.4444      6.285      1      NOPRINT
13.6111	13.308	4.4444      6.804      2      NOPRINT
17.7233	13.263	3.7800      7.281      3      NOPRINT
22.0017	12.915	4.7767      7.628      3      NOPRINT
26.7783	11.532	4.7767      7.511      4      NOPRINT
32.5000	10.162	6.6667      7.224      4      NOPRINT
39.1667	9.011	6.6667      6.877      5      NOPRINT
45.8333	7.795	6.6667      6.466      6      NOPRINT
52.5000	6.544	6.6667      6.039      6      NOPRINT
59.1667	5.361	6.6667      5.631      7      NOPRINT
65.8333	4.188	6.6667      5.223      7      NOPRINT
72.5000	3.125	6.6667      4.815      8      NOPRINT
79.1667	2.319	6.6667      4.407      8      NOPRINT
85.8333	1.526	6.6667      3.999      8      NOPRINT
91.3889	0.863	4.4444      3.659      8      NOPRINT
95.8333	0.370	4.4444      3.203      8      NOPRINT
100.2778	0.106	4.4444      1.600      8      NOPRINT

### A.5.3 ServoDyn

```

----- SERVODYN V1.01.* INPUT FILE -----
SNL13.2-00-Floating Turbine Design Model SNL 13.2MW Turbine with SNL100-02 Baseline
----- SIMULATION CONTROL -----
False      Echo      - Echo input data to <RootName>.ech (flag)
DEFAULT    DT        - Communication interval for controllers (s)
----- PITCH CONTROL -----
          5  PCMode    - Pitch control mode {0: none, 1: user-defined from routine
          0  TPCOn     - Time to enable active pitch control (s)
        9999.9 TPitManS(1) - Time to start override pitch maneuver for blade 1 and end
        9999.9 TPitManS(2) - Time to start override pitch maneuver for blade 2 and end
        9999.9 TPitManS(3) - Time to start override pitch maneuver for blade 3 and end
          8  PitManRat(1) - Pitch rate at which override pitch maneuver heads toward
          8  PitManRat(2) - Pitch rate at which override pitch maneuver heads toward
          8  PitManRat(3) - Pitch rate at which override pitch maneuver heads toward
        90.0  BLPitchF(1) - Blade 1 final pitch for pitch maneuvers (degrees)
        90.0  BLPitchF(2) - Blade 2 final pitch for pitch maneuvers (degrees)
        90.0  BLPitchF(3) - Blade 3 final pitch for pitch maneuvers (degrees)
----- GENERATOR AND TORQUE CONTROL -----
          5  VSContrl   - Variable-speed control mode {0: none, 1: simple VS,
          2  GenModel   - Generator model {1: simple, 2: Thevenin, 3: user-defined
        94.4  GenEff     - Generator efficiency [ignored by the Thevenin and user
False      GenTiStr    - Method to start the generator {T: timed using TimGenOn
True       GenTiStp    - Method to stop the generator {T: timed using TimGenOf
          2  SpdGenOn   - Generator speed to turn on the generator for a startup
          0  TimGenOn   - Time to turn on the generator for a startup (s)
        9999.9 TimGenOf - Time to turn off the generator (s) [used only when GenTiStp
----- SIMPLE VARIABLE-SPEED TORQUE CONTROL -----
        1173.7 VS_RtGnSp - Rated generator speed for simple variable-speed generator
        115000 VS_RtTq   - Rated generator torque/constant generator torque in Region
          0.03  VS_Rgn2K  - Generator torque constant in Region 2 for simple variable-s
          0.0001 VS_SlPc  - Rated generator slip percentage in Region 2 1/2 for simple
----- SIMPLE INDUCTION GENERATOR -----
        9999.9 SIG_SlPc  - Rated generator slip percentage (%) [used only when VSContrl
        9999.9 SIG_SySp  - Synchronous (zero-torque) generator speed (rpm) [used only
        9999.9 SIG_RtTq  - Rated torque (N-m) [used only when VSContrl=0 and GenModel=1
        9999.9 SIG_PORT  - Pull-out ratio (Tpulout/Trated) (-) [used only when VSCont
----- THEVENIN-EQUIVALENT INDUCTION GENERATOR -----
        9999.9 TEC_Freq   - Line frequency [50 or 60] (Hz) [used only when VSContrl=0
        9998  TEC_NPol   - Number of poles [even integer > 0] (-) [used only when
        9999.9 TEC_SRes  - Stator resistance (ohms) [used only when VSContrl=0 and
        9999.9 TEC_RRes  - Rotor resistance (ohms) [used only when VSContrl=0 and
        9999.9 TEC_VLL   - Line-to-line RMS voltage (volts) [used only when VSContrl=0
        9999.9 TEC_SLR   - Stator leakage reactance (ohms) [used only when VSContrl=0
        9999.9 TEC_RLR   - Rotor leakage reactance (ohms) [used only when VSContrl=0
        9999.9 TEC_MR    - Magnetizing reactance (ohms) [used only when VSContrl=0
----- HIGH-SPEED SHAFT BRAKE -----
          1  HSSBrMode   - HSS brake model {1: simple, 2: user-defined from routine
        9999.9 THSSBrDp  - Time to initiate deployment of the HSS brake (s)
          0.6  HSSBrDT    - Time for HSS-brake to reach full deployment once initiated
        28116.2 HSSBrTqF - Fully deployed HSS-brake torque (N-m)
----- NACELLE-YAW CONTROL -----
          0  YCMode      - Yaw control mode {0: none, 1: simple, 2: user-defined from
        9999.9 TYCOn     - Time to enable active yaw control (s) [unused when YCMode=0]
          0  YawNeut     - Neutral yaw position--yaw spring force is zero at this yaw
        9.02832E+09 YawSpr - Nacelle-yaw spring constant (N-m/rad)

```

```

1.916E+07 YawDamp      - Nacelle-yaw damping constant (N-m/(rad/s))
9999.9    TYawManS    - Time to start override yaw maneuver and end standard yaw
0.3       YawManRat   - Yaw maneuver rate (in absolute value) (deg/s)
0         NacYawF     - Final yaw angle for override yaw maneuvers (degrees)
----- BLADED INTERFACE -----
"DISCON_SNL_win32.dll" DLL_FileName - Name/location of the dynamic library
0 NacYaw_North - Reference yaw angle of the nacelle when the upwind end
0 Ptch_Cntrl   - Record 28: Use individual pitch control {0: collective
0 Ptch_SetPnt - Record 5: Below-rated pitch angle set-point (deg)
0 Ptch_Min     - Record 6: Minimum pitch angle (deg) [used only with
0 Ptch_Max     - Record 7: Maximum pitch angle (deg) [used only with
0 PtchRate_Min - Record 8: Minimum pitch rate (most negative value allow
0 PtchRate_Max - Record 9: Maximum pitch rate (deg/s) [used only with
0 Gain_OM      - Record 16: Optimal mode gain (Nm/(rad/s)^2) [used only
0 GenSpd_MinOM - Record 17: Minimum generator speed (rpm) [used only with
0 GenSpd_MaxOM - Record 18: Optimal mode maximum speed (rpm) [used only
0 GenSpd_Dem   - Record 19: Demanded generator speed above rated (rpm)
0 GenTrq_Dem   - Record 22: Demanded generator torque above rated (Nm)
0 GenPwr_Dem   - Record 13: Demanded power (W) [used only with Bladed
----- BLADED INTERFACE TORQUE-SPEED LOOK-UP TABLE -----
0 DLL_NumTrq   - Record 26: No. of points in torque-speed look-up table
GenSpd_TLU    GenTrq_TLU
(rpm)         (Nm)
----- OUTPUT -----
True          SumPrint   - Print summary data to <RootName>.sum (flag) (currently
1            OutFile     - Switch to determine where output will be placed:
True         TabDelim    - Use tab delimiters in text tabular output file? (flag)
"ES10.3E2"    OutFmt     - Format used for text tabular output (except time).
0            TStart      - Time to begin tabular output (s) (currently unused)
            OutList      - The next line(s) contains a list of output parameters.
"GenPwr"      - Electrical generator power and torque
"GenTq"       - Electrical generator power and torque
END of input file (the word "END" must appear in the first 3 columns of this last
-----

```

#### A.5.4 ElastoDyn

```

----- ELASTODYN V1.01.* INPUT FILE -----
SNL13.2-00-Floating Turbine Design Model SNL 13.2MW Turbine with SNL100-02 Baseline
----- SIMULATION CONTROL -----
False        Echo        - Echo input data to "<RootName>.ech" (flag)
3            Method       - Integration method: {1: RK4, 2: AB4, or 3: ABM4} (-)
0.01         DT          - Integration time step (s)
----- ENVIRONMENTAL CONDITION -----
9.80665      Gravity     - Gravitational acceleration (m/s^2)
----- DEGREES OF FREEDOM -----
True         FlapDOF1    - First flapwise blade mode DOF (flag)
True         FlapDOF2    - Second flapwise blade mode DOF (flag)
True         EdgeDOF     - First edgewise blade mode DOF (flag)
False        TeetDOF     - Rotor-teeter DOF (flag) [unused for 3 blades]
True         DrTrDOF     - Drivetrain rotational-flexibility DOF (flag)
True         GenDOF      - Generator DOF (flag)
True         YawDOF      - Yaw DOF (flag)
True         TwFADOF1    - First fore-aft tower bending-mode DOF (flag)
True         TwFADOF2    - Second fore-aft tower bending-mode DOF (flag)

```

True	TwSSDOF1	- First side-to-side tower bending-mode DOF (flag)
True	TwSSDOF2	- Second side-to-side tower bending-mode DOF (flag)
True	PtfmSgDOF	- Platform horizontal surge translation DOF (flag)
True	PtfmSwDOF	- Platform horizontal sway translation DOF (flag)
True	PtfmHvDOF	- Platform vertical heave translation DOF (flag)
True	PtfmRDOF	- Platform roll tilt rotation DOF (flag)
True	PtfmPDOF	- Platform pitch tilt rotation DOF (flag)
True	PtfmYDOF	- Platform yaw rotation DOF (flag)
----- INITIAL CONDITIONS -----		
	0	OoPDefl - Initial out-of-plane blade-tip displacement (meters)
	0	IPDefl - Initial in-plane blade-tip deflection (meters)
	0	BlPitch(1) - Blade 1 initial pitch (degrees)
	0	BlPitch(2) - Blade 2 initial pitch (degrees)
	0	BlPitch(3) - Blade 3 initial pitch (degrees) [unused for 2 blades]
	0	TeetDefl - Initial or fixed teeter angle (degrees) [unused for
	0	Azimuth - Initial azimuth angle for blade 1 (degrees)
7.46	RotSpeed	- Initial or fixed rotor speed (rpm)
0	NacYaw	- Initial or fixed nacelle-yaw angle (degrees)
0	TTDspFA	- Initial fore-aft tower-top displacement (meters)
0	TTDspSS	- Initial side-to-side tower-top displacement (meters)
0	PtfmSurge	- Initial or fixed horizontal surge translational
0	PtfmSway	- Initial or fixed horizontal sway translational
0	PtfmHeave	- Initial or fixed vertical heave translational
0	PtfmRoll	- Initial or fixed roll tilt rotational displacement of
0	PtfmPitch	- Initial or fixed pitch tilt rotational displacement of
0	PtfmYaw	- Initial or fixed yaw rotational displacement of
----- TURBINE CONFIGURATION -----		
3	NumBl	- Number of blades (-)
102.5	TipRad	- The distance from the rotor apex to the blade tip
2.5	HubRad	- The distance from the rotor apex to the blade root
-2.5	PreCone(1)	- Blade 1 cone angle (degrees)
-2.5	PreCone(2)	- Blade 2 cone angle (degrees)
-2.5	PreCone(3)	- Blade 3 cone angle (degrees) [unused for 2 blades]
0	HubCM	- Distance from rotor apex to hub mass
0	UndSling	- Undersling length [distance from teeter pin to the
0	Delta3	- Delta-3 angle for teetering rotors (degrees) [unused
0	AzimB1Up	- Azimuth value to use for I/O when blade 1 points up
-8.16114	OverHang	- Distance from yaw axis to rotor apex [3 blades] or
1.912	ShftGagL	- Distance from rotor apex [3 blades] or teeter
-5	ShftTilt	- Rotor shaft tilt angle (degrees)
3.09	NacCMxn	- Downwind distance from the tower-top to the nacelle
0	NacCMyn	- Lateral distance from the tower-top to the nacelle
2.85	NacCMzn	- Vertical distance from the tower-top to the nacelle
-3.09528	NcIMUxn	- Downwind distance from the tower-top to the nacelle
0	NcIMUyn	- Lateral distance from the tower-top to the nacelle
2.23336	NcIMUzn	- Vertical distance from the tower-top to the nacelle
3.19115	Twr2Shft	- Vertical distance from the tower-top to the rotor
142.4	TowerHt	- Height of tower above ground level [onshore] or MSL
18	TowerBsHt	- Height of tower base above ground level [onshore] or
0	PtfmCMxt	- Downwind distance from the ground level [onshore] or
0	PtfmCMyt	- Lateral distance from the ground level [onshore] or
-15.58584	PtfmCMzt	- Vertical distance from the ground level [onshore] or
0	PtfmRefzt	- Vertical distance from the ground level [onshore] or
----- MASS AND INERTIA -----		
0	TipMass(1)	- Tip-brake mass, blade 1 (kg)
0	TipMass(2)	- Tip-brake mass, blade 2 (kg)

```

0 TipMass(3) - Tip-brake mass, blade 3 (kg) [unused for 2 blades]
245000 HubMass - Hub mass (kg)
812000 HubIner - Hub inertia about rotor axis [3 blades] or teeter axis
3740 GenIner - Generator inertia about HSS (kg m^2)
1.03E+06 NacMass - Nacelle mass (kg)
1.83E+07 NacYIner - Nacelle inertia about yaw axis (kg m^2)
0 YawBrMass - Yaw bearing mass (kg)
2.335491376E7 PtfmMass - Platform mass (kg) ! Metal mass of the platform
4.840940946E10 PtfmRIner - Platform inertia for roll tilt rotation about
4.840940946E10 PtfmPIner - Platform inertia for pitch tilt rotation about
8.016775675E10 PtfmYIner - Platform inertia for yaw rotation about the platform
----- BLADE -----
"SNL100-02_FASTBlade_precomp.dat" BldFile(1) - Name of file containing properties
"SNL100-02_FASTBlade_precomp.dat" BldFile(2) - Name of file containing properties
"SNL100-02_FASTBlade_precomp.dat" BldFile(3) - Name of file containing properties
----- ROTOR-TEETER -----
0 TeetMod - Rotor-teeter spring/damper model {0: none, 1: standard}
0 TeetDmpP - Rotor-teeter damper position (degrees) [used only for
0 TeetDmp - Rotor-teeter damping constant (N-m/(rad/s)) [used only
0 TeetCDmp - Rotor-teeter rate-independent Coulomb-damping moment
0 TeetSStP - Rotor-teeter soft-stop position (degrees) [used only
0 TeetHStP - Rotor-teeter hard-stop position (degrees) [used only
0 TeetSSSp - Rotor-teeter soft-stop linear-spring constant (N-m/rad)
0 TeetHSSp - Rotor-teeter hard-stop linear-spring constant (N-m/rad)
----- DRIVETRAIN -----
100 GBxEff - Gearbox efficiency (%)
157.8 GBRatio - Gearbox ratio (-)
8.67637E+08 DTTorSpr - Drivetrain torsional spring (N-m/rad)
6.215E+06 DTTorDmp - Drivetrain torsional damper (N-m/(rad/s))
----- FURLING -----
False Furling - Read in additional model properties for furling
"unused" FurlFile - Name of file containing furling properties
----- TOWER -----
20 TwrNodes - Number of tower nodes used for analysis (-)
"SNL13pt2_Floating_Tower.dat" TwrFile - Name of file containing tower
----- OUTPUT -----
True SumPrint - Print summary data to "<RootName>.sum" (flag)
2 OutFile - Switch to determine where output will be placed:
True TabDelim - Use tab delimiters in text tabular output file? (flag)
"ES10.3E2" OutFmt - Format used for text tabular output (except time).
0 TStart - Time to begin tabular output (s) (currently unused)
1 DecFact - Decimation factor for tabular output {1: output every
0 NTwGages - Number of tower nodes that have strain gages for output
10 TwrGagNd - List of tower nodes that have strain gages [1 to TwrNod
3 NB1Gages - Number of blade nodes that have strain gages for output
5,10,14 BldGagNd - List of blade nodes that have strain gages [1 to BldNo
OutList - The next line(s) contains a list of output parameters.
RotSpeed - Low-speed shaft speed
GenSpeed - High-speed shaft speed
OoPDefl1 - Blade 1 out-of-plane deflection
IPDefl1 - Blade 1 in-plane deflection
TwstDefl1 - Blade 1 tip twist
BldPitch1 - Blade 1 pitch angle
TTDspFA - Tower fore-aft deflection
TTDspSS - Tower side-to-side deflection
TTDspTwst - Tower top twist

```



```

PtfmSurge          - Platform translational surge displacement
PtfmSway           - Platform translational sway displacement
PtfmHeave          - Platform translational heave displacement
PtfmRoll           - Platform rotational roll displacement
PtfmPitch          - Platform rotational pitch displacement
PtfmYaw            - Platform rotational yaw displacement
RootFxc1           - Out-of-plane shear force at the root of blade 1
RootFyc1           - In-plane shear force at the root of blade 1
RootFzc1           - Axial force at the root of blade 1
RootMxc1           - In-plane bending moment at the root of blade 1
RootMyc1           - Out-of-plane bending moment at the root of blade 1
RootMzc1           - Pitching moment at the root of blade 1
RotTorq            - Rotor torque
LSSGagMya          - Low-speed shaft 0- rotating bending moments at the
LSSGagMza          - Low-speed shaft 90-rotating bending moments at the
YawBrFxp           - Fore-aft shear force at the top of the tower
YawBrFyp           - Side-to-side shear force at the top of the tower
YawBrFzp           - Vertical force at the top of the tower
YawBrMxp           - Side-to-side bending moment at the top of the tower
YawBrMyp           - Fore-aft bending moment at the top of the tower
YawBrMzp           - Yaw moment at the top of the tower
TwrBsFxt           - Fore-aft shear force at the base of the tower
TwrBsFyt           - Side-to-side shear force at the base of the tower
TwrBsFzt           - Vertical force at the base of the tower
TwrBsMxt           - Side-to-side bending moment at the base of the tower
TwrBsMyt           - Fore-aft bending moment at the base of the tower
TwrBsMzt           - Yaw moment at the base of the tower
END of input file (the word "END" must appear in the first 3 columns of this last
-----

```

### A.5.5 Blade File for ElastoDyn

```

----- ELASTODYN V1.00.* INDIVIDUAL BLADE INPUT FILE -----
Properties generated using NuMAD2PreComp2FASTBlade on 20-Nov-2013
----- BLADE PARAMETERS -----
      34  NBlInpSt  - Number of blade input stations (-)
      1.5  BldFlDmp(1) - Blade flap mode #1 structural damping in percent
      1.5  BldFlDmp(2) - Blade flap mode #2 structural damping in percent
      1.5  BldEdDmp(1) - Blade edge mode #1 structural damping in percent
----- BLADE ADJUSTMENT FACTORS -----
      1  FlStTunr(1) - Blade flapwise modal stiffness tuner, 1st mode (-)
      1  FlStTunr(2) - Blade flapwise modal stiffness tuner, 2nd mode (-)
      1  AdjBlMs    - Factor to adjust blade mass density (-)
      1  AdjFlSt    - Factor to adjust blade flap stiffness (-)
      1  AdjEdSt    - Factor to adjust blade edge stiffness (-)
----- DISTRIBUTED BLADE PROPERTIES -----
      BlFract      PitchAxis      StrcTwst      BMassDen      FlpStff      EdgStff
      (-)          (-)            (deg)        (kg/m)        (Nm^2)       (Nm^2)
0.0000000E+00  2.5000000E-01  1.3310000E+01  3.6000000E+03  2.1030000E+11  2.0740000E+11
5.0000000E-03  2.5000000E-01  1.3310000E+01  2.9700000E+03  1.7530000E+11  1.7150000E+11
7.0000000E-03  2.5000000E-01  1.3310000E+01  2.5960000E+03  1.5270000E+11  1.4970000E+11
9.0000000E-03  2.5000000E-01  1.3310000E+01  2.2230000E+03  1.2940000E+11  1.2790000E+11
1.1000000E-02  2.5000000E-01  1.3310000E+01  1.8540000E+03  1.0800000E+11  1.0630000E+11
1.3000000E-02  2.5000000E-01  1.3310000E+01  1.6920000E+03  1.0210000E+11  9.6160000E+10
2.4000000E-02  2.5100000E-01  1.3310000E+01  1.7430000E+03  9.5620000E+10  9.0580000E+10

```

```

2.6000000E-02  2.5200000E-01  1.3310000E+01  1.6280000E+03  8.8060000E+10  8.3170000E+10
4.7000000E-02  2.9800000E-01  1.3310000E+01  1.6010000E+03  8.0970000E+10  8.3230000E+10
6.8000000E-02  3.1800000E-01  1.3310000E+01  1.6120000E+03  7.9110000E+10  8.7930000E+10
8.9000000E-02  3.4300000E-01  1.3310000E+01  1.3650000E+03  6.7190000E+10  8.1940000E+10
1.1400000E-01  3.7500000E-01  1.3310000E+01  1.1950000E+03  5.7380000E+10  7.3460000E+10
1.4600000E-01  3.7500000E-01  1.3310000E+01  7.8050000E+02  4.6840000E+10  4.1320000E+10
.
.
1.0000000E+00  3.7500000E-01  0.0000000E+00  4.6720000E+00  3.3240000E+03  4.4470000E+04
----- BLADE MODE SHAPES -----
    0.335565  BldFl1Sh(2) - Flap mode 1, coeff of x^2
    0.887432  BldFl1Sh(3) - , coeff of x^3
   -0.384559  BldFl1Sh(4) - , coeff of x^4
    0.47486   BldFl1Sh(5) - , coeff of x^5
   -0.313298  BldFl1Sh(6) - , coeff of x^6
   -1.54759   BldFl2Sh(2) - Flap mode 2, coeff of x^2
    5.43068   BldFl2Sh(3) - , coeff of x^3
   -18.7877   BldFl2Sh(4) - , coeff of x^4
    26.1907   BldFl2Sh(5) - , coeff of x^5
   -10.286    BldFl2Sh(6) - , coeff of x^6
    0.827781  BldEdgSh(2) - Edge mode 1, coeff of x^2
   -0.693626  BldEdgSh(3) - , coeff of x^3
    3.2853    BldEdgSh(4) - , coeff of x^4
   -3.59026   BldEdgSh(5) - , coeff of x^5
    1.17081   BldEdgSh(6) - , coeff of x^6
(File available upon request)

```

## A.5.6 Tower File for ElastoDyn

```

----- ELASTODYN V1.00.* TOWER INPUT FILE -----
SNL13.2-00-Land tower input properties.
----- TOWER PARAMETERS -----
    11  NTwInpSt  - Number of input stations to specify tower geometry
     1  TwrFADmp(1) - Tower 1st fore-aft mode structural damping ratio (%)
     1  TwrFADmp(2) - Tower 2nd fore-aft mode structural damping ratio (%)
     1  TwrSSDmp(1) - Tower 1st side-to-side mode structural damping ratio
     1  TwrSSDmp(2) - Tower 2nd side-to-side mode structural damping ratio
----- TOWER ADJUSTMUNT FACTORS -----
     1  FASStTunr(1) - Tower fore-aft modal stiffness tuner, 1st mode (-)
     1  FASStTunr(2) - Tower fore-aft modal stiffness tuner, 2nd mode (-)
     1  SSSStTunr(1) - Tower side-to-side stiffness tuner, 1st mode (-)
     1  SSSStTunr(2) - Tower side-to-side stiffness tuner, 2nd mode (-)
  2.6471 AdjTwMa  - Factor to adjust tower mass density (-)
   7.007 AdjFAST  - Factor to adjust tower fore-aft stiffness (-)
   7.007 AdjSSSt  - Factor to adjust tower side-to-side stiffness (-)
----- DISTRIBUTED TOWER PROPERTIES -----
    HtFract      TMassDen      TwFAStif      TwSSStif
    (-)          (kg/m)        (Nm^2)        (Nm^2)
0.0000000E+00  5.5908700E+03  6.1434300E+11  6.1434300E+11
1.0000000E-01  5.2324300E+03  5.3482100E+11  5.3482100E+11
2.0000000E-01  4.8857600E+03  4.6326700E+11  4.6326700E+11
3.0000000E-01  4.5508700E+03  3.9913100E+11  3.9913100E+11
4.0000000E-01  4.2277500E+03  3.4188300E+11  3.4188300E+11
.
.

```

```

1.0000000E+00  2.5362700E+03  1.1582000E+11  1.1582000E+11
----- TOWER FORE-AFT MODE SHAPES -----
    0.7324 TwFAM1Sh(2) - Mode 1, coefficient of x^2 term
    2.226 TwFAM1Sh(3) -      , coefficient of x^3 term
   -5.753 TwFAM1Sh(4) -      , coefficient of x^4 term
    6.3097 TwFAM1Sh(5) -      , coefficient of x^5 term
   -2.5151 TwFAM1Sh(6) -      , coefficient of x^6 term
  -63.2276 TwFAM2Sh(2) - Mode 2, coefficient of x^2 term
   49.8201 TwFAM2Sh(3) -      , coefficient of x^3 term
    9.4686 TwFAM2Sh(4) -      , coefficient of x^4 term
   40.5872 TwFAM2Sh(5) -      , coefficient of x^5 term
  -35.6482 TwFAM2Sh(6) -      , coefficient of x^6 term
----- TOWER SIDE-TO-SIDE MODE SHAPES -----
    1.4671 TwSSM1Sh(2) - Mode 1, coefficient of x^2 term
   -1.893 TwSSM1Sh(3) -      , coefficient of x^3 term
    3.2397 TwSSM1Sh(4) -      , coefficient of x^4 term
   -2.4408 TwSSM1Sh(5) -      , coefficient of x^5 term
    0.627 TwSSM1Sh(6) -      , coefficient of x^6 term
  -33.9372 TwSSM2Sh(2) - Mode 2, coefficient of x^2 term
    4.6261 TwSSM2Sh(3) -      , coefficient of x^3 term
   59.8334 TwSSM2Sh(4) -      , coefficient of x^4 term
  -21.6117 TwSSM2Sh(5) -      , coefficient of x^5 term
   -7.9107 TwSSM2Sh(6) -      , coefficient of x^6 term
(File available upon request)

```

## A.5.7 HydroDyn

```

----- HydroDyn v2.01.* Input File -----
SNL13.2-00-Floating Turbine Design Model SNL 13.2MW Turbine with SNL100-02 Baseline
False      Echo      - Echo the input file data (flag)
----- ENVIRONMENTAL CONDITIONS -----
1025      WtrDens      - Water density (kg/m^3)
200      WtrDpth      - Water depth (meters)
0      MSL2SWL      - Offset between still-water level and mean sea
----- WAVES -----
2      WaveMod      - Incident wave kinematics model {0: none=still
0      WaveStMod      - Model for stretching incident wave kinematics to
4000.0      WaveTMax      - Analysis time for incident wave calculations (sec)
0.2      WaveDT      - Time step for incident wave calculations (sec)
5.5      WaveHs      - Significant wave height of incident waves (meters)
11.00      WaveTp      - Peak-spectral period of incident waves (sec)
"DEFAULT"      WavePkShp      - Peak-shape parameter of incident wave spectrum (-)
0.314159      WvLowCOff      - Low cut-off frequency or lower frequency limit of
1.570796      WvHiCOff      - High cut-off frequency or upper frequency limit of
0      WaveDir      - Incident wave propagation heading direction
0      WaveDirMod      - Directional spreading function {0: none, 1: COS2S}
1      WaveDirSpread      - Wave direction spreading coefficient ( > 0 )
1      WaveNDir      - Number of wave directions
0      WaveDirRange      - Range of wave directions (full range: WaveDir +/-
1734175506      WaveSeed(1)      - First random seed of incident waves [-2147483648
1972637277      WaveSeed(2)      - Second random seed of incident waves [-2147483648
FALSE      WaveNDamp      - Flag for normally distributed amplitudes (flag)
""      GHWvFile      - Root name of GH Bladed files containing wave data
1      NWaveElev      - Number of points where the incident wave elevation
0      WaveElevxi      - List of xi-coordinates for points where the incid

```

```

0          WaveElevyi      - List of yi-coordinates for points where the incid
----- 2ND-ORDER WAVES -----
False      WvMnDrift       - Mean-drift                               2nd-order wave kinemati
False      WvDiffQTF       - Full difference-frequency 2nd-order wave kinemati
False      WvSumQTF        - Full summation-frequency 2nd-order wave kinemati
0          WvLowCoffD      - Low frequency cutoff used in the difference-frequencies (rad/s)
500        WvHiCoffD      - High frequency cutoff used in the difference-frequencies (rad/s)
0          WvLowCoffS      - Low frequency cutoff used in the summation-frequencies (rad/s)
500        WvHiCoffS      - High frequency cutoff used in the summation-frequencies (rad/s)
----- CURRENT -----
0          CurrMod         - Current profile model {0: none=no current, 1: standard, 2: user
0          CurrSSVO        - Sub-surface current velocity at still water level (m/s)
"DEFAULT" CurrSSDir       - Sub-surface current heading direction (degrees) or
20         CurrNSRef       - Near-surface current reference depth (meters)
0          CurrNSVO        - Near-surface current velocity at still water level (m/s)
0          CurrNSDir       - Near-surface current heading direction (degrees)
0          CurrDIV         - Depth-independent current velocity (m/s)
0          CurrDIDir       - Depth-independent current heading direction (degrees)
----- FLOATING PLATFORM -----
TRUE       HasWAMIT        - Using WAMIT (flag)
"HydroData\snl_semi"     WAMITFile    - Root name of WAMIT output files containing
1          WAMITULEN       - Characteristic body length scale used to redimensionalize WAMIT
81163.944 PtfmVol0        - Displaced volume of water when the platform is in its
0          PtfmCOBxt       - The xt offset of the center of buoyancy (COB) from the platform
0          PtfmCOByt       - The yt offset of the center of buoyancy (COB) from the platform
1          RdtnMod         - Radiation memory-effect model {0: no memory-effect calculation,
60         RdtnTMax        - Analysis time for wave radiation kernel calculations (sec)
DEFAULT    RdtnDT         - Time step for wave radiation kernel calculations (sec)
----- 2ND-ORDER FLOATING PLATFORM FORCES -----
0          MnDrift         - Mean-drift 2nd-order forces computed
0          NewmanApp       - Slow-drift 2nd-order forces computed with Newman's approximation
0          DiffQTF         - Full difference-frequency 2nd-order forces computed with full
0          SumQTF          - Full summation -frequency 2nd-order forces computed with full
----- FLOATING PLATFORM FORCE FLAGS -----
True       PtfmSgF         - Platform horizontal surge translation force (flag)
True       PtfmSwF         - Platform horizontal sway translation force (flag)
True       PtfmHvF         - Platform vertical heave translation force (flag)
True       PtfmRF          - Platform roll tilt rotation force (flag)
True       PtfmPF          - Platform pitch tilt rotation force (flag)
True       PtfmYF          - Platform yaw rotation force (flag)
----- PLATFORM ADDITIONAL STIFFNESS AND DAMPING -----
0          0              0              0              0              0          AddFO
0          0              0              0              0              0          AddCLin
0          0              0              0              0              0
0          0              0              0              0              0
0          0              0          1.52351553E10          0              0
0          0              0              0          1.52351553E10          0
0          0              0              0              0              0
0          0              0              0              0              0          AddBLin
0          0              0              0              0              0
0          0              0              0              0              0
0          0              0              0              0              0
0          0              0              0              0              0
0          0              0              0              0              0
0          0              0              0              0              0
0          0              0              0              0              0          AddBQuad
0          0              0              0              0              0

```

0	0	0	0	0	0
0	0	0	0	0	0
0	0	0	0	0	0
0	0	0	0	0	0

----- AXIAL COEFFICIENTS -----

2 NAXCoef - Number of axial coefficients (-)

AxCoefID	AxCd	AxCa	AxCp
(-)	(-)	(-)	(-)
1	0.00	0.00	1.00
2	9.60	0.00	1.00

----- MEMBER JOINTS -----

44 NJoints - Number of joints (-) [must be exactly 0 or at least 2]

JointID	Jointxi	Jointyi	Jointzi	JointAxID	JointOvrld	[JointOvrld]
(-)	(m)	(m)	(m)	(-)	(switch)	
1	0.00000	0.00000	-36.00000	1	0	
2	0.00000	0.00000	18.00000	1	0	
3	25.98077	45.00000	-25.20000	1	0	
4	25.98077	45.00000	21.60000	1	0	
5	-51.96152	0.00000	-25.20000	1	0	
6	-51.96152	0.00000	21.60000	1	0	
7	25.98077	-45.00000	-25.20000	1	0	
8	25.98077	-45.00000	21.60000	1	0	
.						
.						
44	25.98077	-45.00000	-35.89200	1	0	

----- MEMBER CROSS-SECTION PROPERTIES -----

4 NPropSets - Number of member property sets (-)

PropSetID	PropD	PropThck	
(-)	(m)	(m)	
1	11.70000	0.03000	! Main Column
2	21.60000	0.0600	! Upper Columns
3	43.20000	0.0600	! Base Columns
4	2.88000	0.01750	! pontoons

----- SIMPLE HYDRODYNAMIC COEFFICIENTS (model 1) -----

SimplCd	SimplCdMG	SimplCa	SimplCaMG	SimplCp	SimplCpMG
(-)	(-)	(-)	(-)	(-)	(-)
0.00	0.00	0.00	0.00	1.00	1.00

----- DEPTH-BASED HYDRODYNAMIC COEFFICIENTS (model 2) -----

0 NCoefDpth - Number of depth-dependent coefficients (-)

Dpth	DpthCd	DpthCdMG	DpthCa	DpthCaMG	DpthCp	DpthCpMG
(m)	(-)	(-)	(-)	(-)	(-)	(-)

----- MEMBER-BASED HYDRODYNAMIC COEFFICIENTS (model 3) -----

25 NCoefMembers - Number of member-based coefficients (-)

MemberID	MemberCd1	MemberCd2	MemberCdMG1	MemberCdMG2	MemberCa1
MemberCa2	MemberCaMG1	MemberCaMG2	MemberCp1	MemberCp2	MemberCpMG1
MemberCpMG2	MemberAxCa1	MemberAxCa2	MemberAxCaMG1	MemberAxCaMG2	MemberAxCp1
MemberAxCp2	MemberAxCpMG1	MemberAxCpMG2			

Main Column ...  
Upper Column 1 ...  
Upper Column 2 ...  
Upper Column 3 ...  
Base Column 1 ...  
Base Column 2 ...  
Base Column 3 ...  
Base column cap 1 ...  
Base column cap 2 ...

Base column cap 3 ...  
Delta Pontoon, Upper 1 ...  
Delta Pontoon, Upper 2 ...  
Delta Pontoon, Upper 3 ...  
Delta Pontoon, Lower 1 ...  
Delta Pontoon, Lower 2 ...  
Delta Pontoon, Lower 3 ...  
Pontoon, Upper 1 ...  
Pontoon, Upper 2 ...  
Pontoon, Upper 3 ...  
Pontoon, Lower 1 ...  
Pontoon, Lower 2 ...  
Pontoon, Lower 3 ...  
Cross Brace 1 ...  
Cross Brace 2 ...  
Cross Brace 3 ...

```

----- MEMBERS -----
25  NMembers      - Number of members (-)
MemberID  MJointID1  MJointID2  MPropSetID1  MPropSetID2  MDivSize  MCoefMod
(-)        (-)        (-)        (-)        (-)        (m)      (switch)  (flag)
1   1   2   1   1   1.0000   3   TRUE          ! Main Column
2   3   4   2   2   1.0000   3   TRUE          ! Upper Column 1
3   5   6   2   2   1.0000   3   TRUE          ! Upper Column 2
.
.
22  40  41  4   4   1.0000   3   TRUE          ! Cross Brace 3
----- FILLED MEMBERS -----
2   NFillGroups    - Number of filled member groups (-) [If FillDens = DEFAULT,
FillNumM  FillMList      FillFSLoc      FillDens
(-)        (-)        (m)        (kg/m^3)
3   2   3   4   -11.106      1025
3   5   6   7   -26.802      1025
----- MARINE GROWTH -----
0   NMGDepths      - Number of marine-growth depths specified (-)
MGDpth    MGThck      MGDens
(m)        (m)        (kg/m^3)
----- MEMBER OUTPUT LIST -----
0   NMOutputs      - Number of member outputs (-) [must be < 10]
MemberID  NOutLoc      NodeLocs [NOutLoc < 10; node locations are normalized
(-)        (-)        (-)
----- JOINT OUTPUT LIST -----
0   NJOutputs      - Number of joint outputs [Must be < 10]
0   JOutLst        - List of JointIDs which are to be output (-)[unused if
----- OUTPUT -----
True      HDSum      - Output a summary file [flag]
False     OutAll     - Output all user-specified member and joint loads
2   OutSwth      - Output requested channels to: [1=Hydrodyn.out, 2=GlueCode.out
"ES11.4e2" OutFmt      - Output format for numerical results (quoted
"A11"      OutSFmt     - Output format for header strings (quoted string)
----- OUTPUT CHANNELS -----
"Wave1Elev"      - Wave elevation at the platform reference point (0,0)
END of output channels and end of file. (the word "END" must appear in the first

```

## A.5.8 MAP

```

----- LINE DICTIONARY -----
LineType      Diam      MassDenInAir      EA      CB
(-)           (m)      (kg/m)           (kN)     (-)
Material      0.13788    351.9612         24.42E5   1.0
-----
Node Type      X      Y      Z      M      B      FX      FY      FZ
(-) (-)      (m)      (m)      (m)      (kg)      (m3)      (kN)      (kN)      (kN)
1  fix      -837.6    0      depth    0      0      #      #      #
2  Vessel   -73.56    0      -25.2     0      0      #      #      #
-----
LINE PROPERTIES
Line  LineType  UnstrLen  NodeAnch  NodeFair  Flags
(-)   (-)      (m)      (-)      (-)      (-)
1      Material  835.35    1          2      fair_tension anch_tension
2      repeat    120 240 0 120 240
-----
SOLVER OPTIONS-----
Option
(-)
-snes_type newtonls
-ksp_type preonly
-msqs_fd_jacobian
-pc_type lu
-pc_factor_nonzeros_along_diagonal
-snes_atol 1e-6
-snes_rtol 1e-12
-snes_stol 1e-6
!
!LRadAnch  LAngAnch  LDpthAnch  LRadFair  LAngFair  LDrftFair
!(m)      (deg)      (m)      (m)      (deg)      (m)
!837.6     60.0      200.0     73.56     60.0      25.2
!837.6     180.0     200.0     73.56     180.0     25.2
!837.6     300.0     200.0     73.56     300.0     25.2
LUnstrLen  LDiam     LMassDen   LEAStff   LSeabedCD LTenTol
(m)        (m)      (kg/m)     (N)      (-)      (-)
835.35     0.13788  351.9612   24.42E8   1.0      0.0000001
835.35     0.13788  351.9612   24.42E8   1.0      0.0000001
835.35     0.13788  351.9612   24.42E8   1.0      0.0000001
-----

```

## Bibliography

- [1] A Robertson, J Jonkman, M Masciola, H Song, A Goupee, A Coulling, and C Luan. Definition of the semisubmersible floating system for Phase II of OC4. *IEA OC4 Report*, 2012.
- [2] H Martin. *Development of a scale model wind turbine for testing of offshore floating wind turbine systems*. PhD thesis, Maine Maritime Academy, 2011.
- [3] J Jonkman. *Dynamics Modeling and Loads Analysis of an Offshore Floating Wind Turbine*. PhD thesis, University of Colorado at Boulder, 2007.
- [4] Large Offshore Rotor Development. <http://energy.sandia.gov/>. Last modified 11-June-2014; accessed 28-July-2014.
- [5] D Griffith and D Ashwill. The Sandia 100-meter all-glass baseline wind turbine blade: SNL100-00. *SAND2011-3779, Sandia National Laboratories, Albuquerque, June*, 2011.
- [6] M Hall. *Mooring line modelling and design optimization of floating offshore wind turbines*. PhD thesis, University of Victoria, 2013.



- [7] NWTC Computer-Aided Engineering Tools (MAP by M Masciola, Ph.D.). <http://wind.nrel.gov/designcodes/simulators/map/>. Last modified 17-July-2014; accessed 28-July-2014.
- [8] C Lee. *WAMIT theory manual*. Massachusetts Institute of Technology, Department of Ocean Engineering, 1995.
- [9] U.S. Energy Information Administration. U.S primary energy production by major source, May 2014.
- [10] European Wind Energy Association. The European offshore wind industry: Key trends and statistics, first half 2014. 2014.
- [11] U.S. Department of Energy. 20% Wind Energy by 2030: Increasing Wind Energys Contribution to U.S. Electricity Supply. 2008.
- [12] D Griffith, D Ashwill, and B Resor. Large offshore rotor development: Design and analysis of the Sandia 100-meter wind turbine blade. In *53rd AIAA Structures, Structural Dynamics, and Materials Conference, Honolulu, HI*, 2012.
- [13] D Matha. Model Development and Loads Analysis of an Offshore Wind Turbine on a Tension Leg Platform with a Comparison to Other Floating Turbine Concepts: April 2009. Technical report, National Renewable Energy Laboratory (NREL), Golden, CO., 2010.

- [14] NWTC Computer-Aided Engineering Tools (FAST by J Jonkman, Ph.D.). <http://wind.nrel.gov/designcodes/simulators/fast/>. Last modified 2-July-2014; accessed 28-July-2014.
- [15] NWTC Computer-Aided Engineering Tools (FAST v8 by J Jonkman, Ph.D. and B Jonkman). <http://wind.nrel.gov/designcodes/simulators/FAST8/>. Last modified 9-July-2014; accessed 28-July-2014.
- [16] J Jonkman and L Buhl Jr. FAST Users guide. 2005.
- [17] B Jonkman. *TurbSim user's guide: Version 1.50*. National Renewable Energy Laboratory Colorado, 2009.
- [18] NWTC Computer-Aided Engineering Tools (TurbSim by N Kelley and B Jonkman). <http://wind.nrel.gov/designcodes/preprocessors/turbsim/>. Last modified 30-May-2013; accessed 28-July-2014.
- [19] AeroHydro Inc. *MultiSurf for WAMIT 8.0 Manual*. 2011.
- [20] International Electrotechnical Commission. Wind Turbines - Part 1: Design Requirements, IEC 61400-1. Technical report, 2007.
- [21] D Griffith and B Resor. Description of Model Data for SNL13.2-00-Land: A 13.2 MW Land-based Turbine Model with SNL100-00 Blades. *Sandia National Laboratories Technical Report, SAND2011-9310P*, 2011.

- [22] D Griffith, B Resor, and D Ashwill. Challenges and opportunities in large offshore rotor development: Sandia 100-meter blade research. In *AWEA WINDPOWER 2012 Conference and Exhibition, Scientific Track Paper, Atlanta, GA, USA*, 2012.
- [23] M Soni. Dynamic Response Analysis of an Offshore Wind Turbine Supported by a Moored Semi-Submersible Platform. Master’s thesis, University of Texas at Austin, 2014.
- [24] D Griffith. The SNL100-01 blade: Carbon design studies for the Sandia 100-meter blade. *Sandia National Laboratories Technical Report, SAND2013-1178*, 1, 2013.
- [25] J Jonkman, S Butterfield, W Musial, and G Scott. *Definition of a 5-MW reference wind turbine for offshore system development*. National Renewable Energy Laboratory Golden, CO, 2009.
- [26] G Nielsen, D Hanson, and B Skaare. Integrated dynamic analysis of floating offshore wind turbines. In *25th International Conference on Offshore Mechanics and Arctic Engineering*, pages 671–679. American Society of Mechanical Engineers, 2006.
- [27] B Skaare, D Hanson, and G Nielsen. Importance of control strategies on fatigue life of floating wind turbines. In *ASME 2007 26th International Conference on Offshore Mechanics and Arctic Engineering*, pages 493–500. American Society of Mechanical Engineers, 2007.

- [28] J Larsen and D Hanson. A method to avoid negative damped low frequent tower vibrations for a floating, pitch controlled wind turbine. In *Journal of Physics: Conference Series*, volume 75, page 012073. IOP Publishing, 2007.
- [29] J Jonkman. *Definition of the Floating System for Phase IV of OC3*. National Renewable Energy Laboratory, 2010.
- [30] S Chakrabarti. Physical model testing of floating offshore structures. In *Proc. Int. Symp. Dynamic Positioning Conference*, pages 1–32, 1998.
- [31] T Ishihara, P Phuc, H Sukegawa, K Shimada, and T Ohyama. A study on the dynamic response of a semi-submersible floating offshore wind turbine system Part 1: A water tank test. In *Proceedings of the 12th International Conference*, pages 2511–2518, 2007.
- [32] P Phuc and T Ishihara. A study on the dynamic response of a semi-submersible floating offshore wind turbine system Part 2: numerical simulation. *ICWE12. Cairns, Australia*, pages 959–966, 2007.
- [33] J Jonkman, A Robertson, and G Hayman. *HydroDyn Users Guide and Theory Manual*. National Renewable Energy Laboratory Colorado, 2014.
- [34] E Lewis. Principles of naval architecture second revision. *Jersey: SNAME*, 1988.
- [35] O Faltinsen. *Sea loads on ships and offshore structures*, volume 1. Cambridge university press, 1993.

- [36] K Hasselmann, T Barnett, E Bouws, H Carlson, D Cartwright, K Enke, J Ewing, H Gienapp, D Hasselmann, P Kruseman, et al. Measurements of wind-wave growth and swell decay during the Joint North Sea Wave Project (JONSWAP). 1973.
- [37] European Wind Energy Association. Wind in power, 2013 European statistics. 2014.
- [38] International Electrotechnical Commission. Wind Turbines - Part 3: Design Requirements for Offshore Wind Turbines, IEC 61400-3. Technical report, 2007.
- [39] A Coulling, A Goupee, A Robertson, J Jonkman, and H Dagher. Validation of a FAST semi-submersible floating wind turbine numerical model with DeepCwind test data. *Journal of Renewable and Sustainable Energy*, 5(2):023116, 2013.
- [40] H Bagbanci. Dynamic analysis of offshore floating wind turbines. Master’s thesis, Instituto Superior Técnico, 2011.

## Vita

Watsamon Sahasakkul was born in Bangkok, Thailand, the daughter of Mr. Surachai Sahasakkul and Mrs. Phenjan Sahasakkul. She received the degree of Bachelor of Engineering from Chulalongkorn University in 2011. She entered the Master's program at the Department of Civil, Architectural, and Environmental Engineering at the University of Texas at Austin in 2012.

Email address: watsamonsahasakkul@utexas.edu

This thesis was typeset with L<sup>A</sup>T<sub>E</sub>X<sup>†</sup> by the author.

---

<sup>†</sup>L<sup>A</sup>T<sub>E</sub>X is a document preparation system developed by Leslie Lamport as a special version of Donald Knuth's T<sub>E</sub>X Program.